

1-1-1976

Design for creep in pressure vessels.

Antonio Serrano Perez

Follow this and additional works at: <http://preserve.lehigh.edu/etd>



Part of the [Mechanical Engineering Commons](#)

Recommended Citation

Perez, Antonio Serrano, "Design for creep in pressure vessels." (1976). *Theses and Dissertations*. Paper 2027.

This Thesis is brought to you for free and open access by Lehigh Preserve. It has been accepted for inclusion in Theses and Dissertations by an authorized administrator of Lehigh Preserve. For more information, please contact preserve@lehigh.edu.

DESIGN FOR CREEP IN PRESSURE VESSELS

by

Antonio Serrano Perez

A Thesis

Presented to the Graduate Committee

of Lehigh University

in Candidacy for the Degree of

Master of Science

in

Mechanical Engineering

Lehigh University

1976

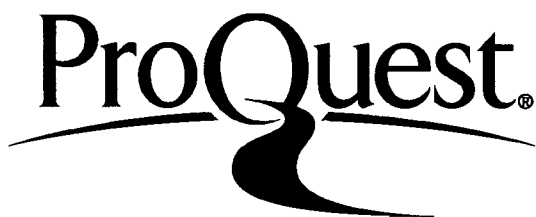
ProQuest Number: EP76300

All rights reserved

INFORMATION TO ALL USERS

The quality of this reproduction is dependent upon the quality of the copy submitted.

In the unlikely event that the author did not send a complete manuscript and there are missing pages, these will be noted. Also, if material had to be removed, a note will indicate the deletion.



ProQuest EP76300

Published by ProQuest LLC (2015). Copyright of the Dissertation is held by the Author.

All rights reserved.

This work is protected against unauthorized copying under Title 17, United States Code
Microform Edition © ProQuest LLC.

ProQuest LLC.
789 East Eisenhower Parkway
P.O. Box 1346
Ann Arbor, MI 48106 - 1346

This Thesis is accepted and approved in partial fulfillment of the requirements for the degree of Master of Science in Mechanical Engineering.

May 5, 1976
(Date)

Professor in Charge

Chairman of Mechanical
Engineering Department

ACKNOWLEDGMENT

This work was conducted in the Department of Mechanical Engineering and Mechanics of Lehigh University, Bethlehem, Pennsylvania.

The author wishes to thank Dr. Arturs Kalnins, Project Director, for his patience, help, technical assistance, and necessary guidance during the development of this project, and for the permission to use his computer program for the stress analysis of axisymmetric shells.

TABLE OF CONTENTS

TITLE PAGE	i
CERTIFICATE OF APPROVAL	ii
ACKNOWLEDGMENT	iii
TABLE OF CONTENTS	iv
ABSTRACT	1
1. INTRODUCTION	2
1.1 Creep Behavior	2
1.2 Importance	3
1.3 Applications	4
2. CREEP VARIABLES	6
2.1 Representation of Creep Data	6
3. CREEP STRESS ANALYSIS	10
3.1 Uniaxial Stress and General Conditions	10
3.2 Multiaxial Stress	12
3.2.1 General Equations	13
3.2.2 Soderberg Approach	17
3.2.3 Bailey Approach	19
3.2.4 Maximun Shear Stress Approach	20
3.3 Creep Rates under Biaxial Stress	22
4. CREEP IN PRESSURE VESSELS	24
4.1 General Considerations	24
4.2 Thin-walled Vessels under Internal Pressure	25

4.2.1	Design	25
4.2.1.1	General Considerations	25
4.2.1.2	Temperatures and Design Stress	29
4.2.1.3	Temperatures at which Short-Time Properties are Important and their Design Stresses	31
4.2.1.4	Temperatures at which both Short-Time and Creep properties are important and their Design Stresses	32
4.2.1.5	Temperatures at which Creep Properties are Important and their Design Stresses	33
4.2.2	Design Conditions	35
4.2.2.1	Design Criterion	35
4.2.2.2	Creep Type	36
4.2.2.3	Approach	36
4.2.2.4	Stress State	37
5.	RESULTS	36
6.	DISCUSSION OF RESULTS	39
7.	CONCLUSIONS	41
8.	NOTATIONS	41
9.	LIST OF TABLES	42
10.	LIST OF FIGURES	45
11.	LIST OF REFERENCES	46

12.	Welded Joint Design	79
12.1	Specifications and Joint Conditions	81
12.2	Design Criterion	85
12.3	Stress Calculation	87
12.4	Material	89
12.5	Results	91
13.	WFA	95

ABSTRACT

This study emerged as a result of work assigned by Dr. Arturo Halming, Professor in the Department of Mechanical Engineering and Mechanics at Lehigh University, in relation to the design of a pressure vessel under creep conditions.

In the introduction, the creep phenomenon is explained, the general behavior of the materials under creep conditions is given, the view point is emphasized that a large number of engineering applications require materials and design that is based, wholly or partially, on creep conditions.

Different theories are given that have been proposed for the representation of creep data.

The procedure for creep stress analysis is given for different stress states, which includes the fundamental assumptions of the general equations, the different approaches to calculate creep strain, and the effects of multiaxial stress in thin-walled pressure vessels under creep conditions.

Then, the design for creep in thin-walled pressure vessels is discussed, where general considerations, temperatures and design stress and the specific design conditions, such as design criterion, creep type, approach, and stress state are included.

Finally, a specific design problem is considered in detail with respect to a pressure vessel that might be used in petrochemical industry.

1. INTRODUCTION

1.1 Creep Behavior

Creep is the name given to time dependent strain of solid materials over long periods under load. When a load has been applied (Fig. 1-1) the strain increases with time to the point where failure finally occurs.

After the initial instantaneous strain ϵ_0 , materials often undergo a period of transient response where the strain rate $\dot{\epsilon}$ ($d\epsilon/dt$) decreases with time to a minimum steady-state value which persists for a substantial portion of the material life. The final failure comes after the creep rate increases during the final stage of creep.

For analytical convenience, researchers have separated the creep curve into three stages based upon the similar response of many materials.

The creep strain occurring at a diminishing rate is called primary creep; that occurring at a minimum and almost constant rate, secondary creep; that occurring at an accelerating rate, tertiary creep (Fig. 1-1)(1) (2).

It is characteristic of creep that, if the specimen is unloaded during the test, some of the strain recovers, as shown by the dashed line in Fig. 1-1. Thus, we find that creep phenomena include both permanent and recoverable strain. The permanent effects are analogous to the plastic

flow at high strain rates which characterizes metal-working processes.

Another test which is characteristic of creep studies is the "relaxation" test. A specimen is loaded rapidly to a fixed strain, and the load required to maintain that strain is recorded. The result is shown in Fig. 1-2. It is natural that there should be a close relation between the earlier portion of the creep (primary creep) and the relaxation curves.

Usually, creep is associated with high temperatures, but whether the temperature required is high or not really depends upon the application.

1.2 Importance

A large number of engineering applications require the use of materials and design which must be based, wholly or partially, on creep behavior.

It was believed for a long time that there exists a limiting stress below which creep and consequent dimensional changes would not occur. But, with the improvement of the accuracy of measurements, the undeniable fact has emerged that such a limiting stress does not exist. Hence, it has now become common practice to design for limited service life at elevated temperatures.

The designers of power-plants are forced to consider

operations at higher temperatures in the interest of greater efficiency. This is seen most directly, of course, from the formula for the efficiency E of conversion of heat into work in an ideal engine, operating between two absolute temperatures $T_1 > T_2$ ($E = 1 - T_2/T_1$). It is possible to raise T_1 to make appreciable gains in efficiency, but this also entails higher creep rates for given stresses.

Applying this argument, it is useful to realize that the operation of steam turbines has steadily increased in efficiency because it has been possible to increase the temperatures through new heat-resistant materials. It is true also of gas turbines, jet aircraft, and missiles that an important limit on performance is set by the permissible deformation of working parts under high temperature and stress.

Other basic reason why engineering design must allow for stress analysis for creep at high temperatures is found in the required strength of vessels in which the high temperature is needed for chemical reactions. Quite often, high pressures are also required.

1.3 Applications

The fast growth of the automobile industry required studies of mechanical behavior of steel in thermal cracking equipment which is used for making gasoline, and hence it

was a matter of direct concern to oil refineries to use design design against creep.

Alloys for the exhaust gas turbines had to be produced; creep strength and ductility were required of these materials.

Higher operating temperatures of steam turbines have forced metallurgists to look for new heat-resistant alloys. Such problems also will become more urgent as nuclear power plants gain greater importance. Additional problems arise in such plants which are created by creep and consequent distortion of uranium fuel elements and their cladding materials.

Jet aircraft and guided missiles have directed more attention to stress analysis for creep.

Aerodynamic heating at high speeds can lead to sustained skin temperatures which pose difficult problems for the designer.

A vital problem of aircraft structural design is to achieve optimum strength-to-weight ratio while avoiding the problems of buckling in the skin supporting members. Much effort has been directed toward the development of new light structural metals such as titanium and its alloys in large part because of their creep strength.

The Pressure Vessel Research Committee of the Welding Research Council has conducted investigations on the creep rupture properties of pressure vessels for use in nuclear and petrochemical industries (3).

2. CREEP VARIABLES

2.1 Representation of Creep Data

A number of different expressions have been proposed for the representation of creep tensile curves.

The creep strain at constant stress in metals, at temperatures far below the melting point, is written as:

$$\epsilon_c = \epsilon_0 \log(at + 1) \quad (2a)$$

in which a is a constant and ϵ_0 is the initial creep strain, some of which may be recoverable (4) (5). Creep curves at constant stress, at higher temperatures, are written by expressions of the form:

$$\epsilon_c = \epsilon_0 + \sum_{\substack{i=1 \\ 0 < m_i < 1}} a_i t^{m_i} + \sum_{\substack{j=1 \\ n_j > 1}} b_j t^{n_j} \quad (2b)$$

where m_i, n_j are constants. The coefficients a_i, b_i contain the effects of temperature and stress (6) (7) (8).

Some researchers have tried to represent the creep rate as:

$$\dot{\epsilon}_c = A \sinh \left(\frac{\sigma}{\sigma_0} \right) \quad (2c)$$

where A and σ_0 depend upon temperature (9)

Other workers have been able to represent creep data of almost all pure metals and many solid-solution alloys by plotting:

$$\begin{array}{ccc} \dot{\epsilon}_c & \text{versus} & t e^{\Delta H/RT} \\ \tau_r & \text{versus} & \dot{\epsilon}_c e^{\Delta H/RT} \end{array} \quad (2d)$$

where ΔH may be interpreted as an activation energy, R is the gas constant, and T the absolute temperature. The representation is used above 0.6 the absolute melting temperature (10).

Other researchers have found the stress dependence to be given by a stress-dependent activation energy:

$$\dot{\epsilon}_c = A e^{[\Delta H + f(\sigma)]/RT} \quad (2e)$$

where A is a constant (11) (12).

Many workers have discussed the stress dependence of creep, but the most useful empirical generalization is that minimum creep rates (steady-state creep rates) are represented by the expression:

$$\left(\frac{d\epsilon_c}{dt} \right)_{min} = (\dot{\epsilon}_c)_{min} = B \sigma^n \quad (2-1)$$

where σ is stress and B and n are constants. The two constants depend upon temperature.

A useful approximation for some engineering purposes is the representation of the entire creep by steady-state flow:

$$\dot{\epsilon}_c = B \sigma^n \quad (2-2)$$

It is very important to indicate that small changes in stress, temperature, composition, heat treatment, or method of manufacture may greatly influence creep behavior, and hence a simple empirical expression for the creep data may be adequate for rational design.

The treatment of creep based on data obtained from

constant-stress creep test in uniaxial tension can be used to predict the creep strain in another type of loading.

On the other hand, relaxation test data (Fig. 2-1) (13) (14) and rupture stress data (Fig. 2-2) (15) (16) (17) can correlate with constant-stress creep laws for the calculation of creep strains and stresses for the general case of steady-state and nonsteady state multiaxial creep (18) (19) (20).

2. CREEP STRESS ANALYSIS

2.1 Uniaxial Stress and General Conditions

The treatment of creep, in general, has been based on data obtained from constant-stress test in uniaxial tension. This is the most common type of creep test and enables the creep properties of a material to be studied in the simplest possible manner.

Practical design problems usually involve a more complex stress state than constant-stress uniaxial tension, and thus it is necessary to use the creep data in tension for the general case of steady-state and nonsteady-state multiaxial creep.

It is assumed that tension tests are available for the temperature at which we wish to make the stress analysis and that the data have been extrapolated, if necessary, to the time duration of interest. Unless otherwise stated, the temperature is taken as constant.

The procedure to be followed is basically that of fitting an empirical expression to represent the experimental constant-stress tension-creep data and with certain assumptions applying it to problems of varying combined stresses. As a first step we must decide upon the accuracy with which the expression will represent the data.

As we indicated in the Section 2.1, small changes in

the variables may greatly influence creep behavior, and hence a simple empirical expression for the creep data may be adequate for rational design.

If the creep curves show a well-defined region of steady-state creep, as illustrated in Fig. 3-1, design may often be based on only steady-state creep and a relationship can be written for the strain rate in terms only of stress. In this case the strain rate is assumed to be a function only of stress, and the creep curves are represented by the lines A and B shown in Fig. 3-1. Expressions for the dependence of creep rate on stress have been indicated in the Section 2.1 (Eqs: (2a), (2b), (2c), (2d), (2e), (2-1) and (2-2)). Attempts have been made to justify all these equations on physical grounds, but Eq. (2-2) is usually the easiest to use and normally gives a satisfactory fit to the data except perhaps at low stresses.

The Eq. (2-2) has formed the basis for most creep calculations in the literature. When creep data follow the general shape of Fig. 3-1, and when steady-state creep contributes most of the strain, this type of representation should be quite adequate. An additional simplification is made in many cases by neglecting elastic strain, but this cannot be done in problems involving the relaxation of initial strains by creep.

An upper limit for the creep strain at a given time can be obtained by using the lines C and D in Fig. 3-1 as

approximations to the creep curve. This approach essentially treat transient strain as an instantaneous effect and combined it with any initial plastic strain (Fig. 3-2). The total initial strain can then be represented in the same manner as creep rates, for example, as a power function of stress. We can conclude that this method will improve the accuracy of prediction at longer times and will provide an upper limit for the displacement but will not be satisfactory for accurate predictions in the region of primary creep (Fig. 3-2).

If the steady-state type of representation is inadequate, we must look for another relation (time hardening, strain hardening, recoverable strain included) which will predict the creep rate in terms of other variables in addition to the stress. This relation, which will be obtained from constant-stress tension tests, should also predict the creep rate after a period of varying stress (18).

Even for materials which do show a region of steady-state creep, an accurate strain prediction may require consideration of initial elastic and plastic strains as well as transient creep (Fig. 3-2).

3.2 Multiaxial Stress Analysis

In the stress analysis of elastic systems in equilibrium, the effects of separate stresses can be evaluated

separately and then added to find the effect combined stress system (method of superposition). Under creep conditions, on the other hand, the relationship between stress and strain rate is generally nonlinear and the method of superposition cannot be used. The stresses must be considered as a combined effect, rather than separately, which greatly complicates the creep-stress analysis. In this analysis we consider solutions for the case of steady-state creep (strain rates depending only on the stresses) and assume an isotropic material (the same material properties in all directions). The method of calculation is fairly well confirmed by experiment and is adequate for a large number of engineering applications.

3.2.1 General Equations

In calculations of elastic deformation the history of loading is not important, and the strain at a given time may be related to the stress at that time. However, in nonelastic deformation the history of loading is important, and it is preferable to relate stress to increments of strain. It is convenient, therefore, in development a creep analysis, to work with the strain increments in units time or, in other words, in units of strain rates.

During elastic deformation of most materials (the outstanding exception being rubbery materials), the volume

is not maintained constant. The largely plastic deformation characteristic of steady creep is found in contrast not to involve appreciable volume changes. If the principal axes of strain do not rotate during the creep, it is possible to express the volume constancy by the relation:

$$\left[(1 + \epsilon_1)(1 + \epsilon_2)(1 + \epsilon_3) \right]_{plastic} = 1 \quad (2-1)$$

Which can be written as, $(\epsilon_1 + \epsilon_2 + \epsilon_3)_{plastic} = 0$, if the strain are small compared with unity, which is usually the case. Since we have assumed that the principal strain axes do not rotate during deformation, the preceding expression may be differentiated directly with respect to time to obtain:

$$\dot{\epsilon}_1 + \dot{\epsilon}_2 + \dot{\epsilon}_3 = 0 \quad (2-2)$$

where, $\dot{\epsilon}_1$, $\dot{\epsilon}_2$ and $\dot{\epsilon}_3$ are the creep strain rates. Although the equations in this analysis apply strictly only to cases in which the principal strain directions do not rotate, it seems likely that they will be good approximations even if this is not the case, e.g., in torsion.

Other ways of stating Eq. (3-2) are that Poisson's ratio is 1/2 or that hydrostatic stress has no influence on the strain rates.

The second assumption employed to develop relations between stress and strain rates is that the principal shear-strain rates are proportional to the principal shear stress in the form

$$\frac{\dot{\epsilon}_1 - \dot{\epsilon}_2}{\sigma_1 - \sigma_2} = \frac{\dot{\epsilon}_2 - \dot{\epsilon}_3}{\sigma_2 - \sigma_3} = \frac{\dot{\epsilon}_3 - \dot{\epsilon}_1}{\sigma_3 - \sigma_1} = C \quad (3-3)$$

C is a constant at a given point in the stressed body but may vary from point to point in the body and may change during the test. The validity of Eq. (3-3), applied to strain increments (plasticity) rather than strain rates, has been discussed many times in the literature. It appears that it is, at the moment, sufficiently accurate for a creep analysis. An additional assumption sometimes used is that Mohr's circles of stress and strain rate are similar.

Combining Eqs. (2-2) and (2-3) :

$$\begin{aligned}\dot{\epsilon}_1 &= 2/3 C (\dot{\epsilon}_1 - 1/2 (\dot{\epsilon}_2 + \dot{\epsilon}_3)) \\ \dot{\epsilon}_2 &= 2/3 C (\dot{\epsilon}_2 - 1/2 (\dot{\epsilon}_3 + \dot{\epsilon}_1)) \quad (2-4) \\ \dot{\epsilon}_3 &= 2/3 C (\dot{\epsilon}_3 - 1/2 (\dot{\epsilon}_1 + \dot{\epsilon}_2))\end{aligned}$$

The problem is now one of identifying C, and this requires some knowledge of the creep behavior of the material.

One procedure is to follow the methods developed for the plastic deformation of ductile metals at temperatures below the creep range and define the quantity:

$$\sigma^* = 1/\sqrt{2} \left[(\sigma_1 - \sigma_2)^2 + (\sigma_2 - \sigma_3)^2 + (\sigma_3 - \sigma_1)^2 \right]^{1/2} \quad (3-5)$$

It is often assumed and fairly well confirmed by experiment that σ^* determines the ability of a multiaxial stress state to produce yielding and subsequent plastic flow (21). Corresponding quantities in terms of strain rates and

strains can be defined as:

$$\dot{\epsilon}^* = \sqrt{2}/3 \left[(\dot{\epsilon}_1 - \dot{\epsilon}_2)^2 + (\dot{\epsilon}_2 - \dot{\epsilon}_3)^2 + (\dot{\epsilon}_3 - \dot{\epsilon}_1)^2 \right]^{1/2} \quad (3-5)$$

$$\epsilon^* = \sqrt{2}/3 \left[(\epsilon_1 - \epsilon_2)^2 + (\epsilon_2 - \epsilon_3)^2 + (\epsilon_3 - \epsilon_1)^2 \right]^{1/2} \quad (3-6a)$$

and it has been shown by experiment (22) that in steady-state multiaxial creep:

$$\dot{\epsilon}^* = f(\sigma^*) \quad (3-7)$$

This is the first place at which the analysis has been restricted to steady-state creep (strain rate depending only on stress)

3.2.2 Soderberg Approach

This approach is based on Mises invariant Eqs. (3-5) and (3-6) according to the following considerations (23)

The numerical factors in Eqs. (3-5) and (3-6) are chosen so that in a tension test with stress σ_1 and strain rate $\dot{\epsilon}_1$, $\sigma_1 = \sigma^*$ and $\dot{\epsilon}_1 = \dot{\epsilon}^*$, and thus the relation

strains can be defined as:

$$\dot{\epsilon}^* = \sqrt{2}/3 \left[(\dot{\epsilon}_1 - \dot{\epsilon}_2)^2 + (\dot{\epsilon}_2 - \dot{\epsilon}_3)^2 + (\dot{\epsilon}_3 - \dot{\epsilon}_1)^2 \right]^{1/2} \quad (3-6)$$

$$\epsilon^* = \sqrt{2}/3 \left[(\epsilon_1 - \epsilon_2)^2 + (\epsilon_2 - \epsilon_3)^2 + (\epsilon_3 - \epsilon_1)^2 \right]^{1/2} \quad (3-6a)$$

and it has been shown by experiment (22) that in steady-state multiaxial creep:

$$\dot{\epsilon}^* = f(\sigma^*) \quad (3-7)$$

This is the first place at which the analysis has been restricted to steady-state creep (strain rate depending only on stress)

3.2.2 Soderberg Approach

This approach is based on Mises invariant Eqs. (3-5) and (3-6) according to the following considerations (23)

The numerical factors in Eqs. (3-5) and (3-6) are chosen so that in a tension test with stress σ_1 and strain rate $\dot{\epsilon}_1$, $\sigma_1 = \sigma^*$ and $\dot{\epsilon}_1 = \dot{\epsilon}^*$, and thus the relation

of Eq. (3-7) can be obtained directly from a tension test. Then, combining Eqs. (3-4) and (3-7), $C = 3\dot{\epsilon}^* / 2\sigma^*$ and hence

$$\begin{aligned}\dot{\epsilon}_1 &= \frac{\dot{\epsilon}^*}{\sigma^*} \left(\sigma_1 - 1/2 (\sigma_2 - \sigma_3) \right) \\ \dot{\epsilon}_2 &= \frac{\dot{\epsilon}^*}{\sigma^*} \left(\sigma_2 - 1/2 (\sigma_3 + \sigma_1) \right) \\ \dot{\epsilon}_3 &= \frac{\dot{\epsilon}^*}{\sigma^*} \left(\sigma_3 - 1/2 (\sigma_1 + \sigma_2) \right)\end{aligned}\tag{3-8}$$

Before Eqs. (3-8) can be used to calculate creep strains, a definite relationship has to be inserted instead of Eq. (3-7). As a multiaxial counterpart of Eq. (2-2) we take:

$$\dot{\epsilon}^* = B \sigma^{*n}\tag{3-9}$$

although an expression corresponding to either Eq. (2c) or (2e) could be taken if it gave a better fit to the data.

Combining Eqs. (3-8) and (3-9) leads to

$$\begin{aligned}\dot{\epsilon}_1 &= B \epsilon^*{}^{n-1} \left(\epsilon_1 - 1/2 (\epsilon_2 + \epsilon_3) \right) \\ \dot{\epsilon}_2 &= B \epsilon^*{}^{n-1} \left(\epsilon_2 - 1/2 (\epsilon_3 + \epsilon_1) \right) \\ \dot{\epsilon}_3 &= B \epsilon^*{}^{n-1} \left(\epsilon_3 - 1/2 (\epsilon_1 + \epsilon_2) \right)\end{aligned}\tag{3-10}$$

where ϵ^* is defined by Eq. (3-5), and we are finally in a position to calculate multiaxial creep strains. The solutions are limited in the same way as the constant-strain rate uniaxial analysis indicated in Section 3.1. They are accurate only when steady-state creep predominates. In statically indeterminate problems they will not give information about the relaxation of initial elastic stresses with time but will enable to carry out the calculation of the steady-state stress distribution after relaxation has occurred.

3.2.3 Bailey Approach

This approach presents another method of obtaining creep rates under multiaxial stress. Bailey's equation

(20) corresponding to the first of Eqs. (3-10) is:

$$\epsilon_1 = \frac{B}{2} \dot{\epsilon}^*{}^{2m} \left((\epsilon_1 - \epsilon_2)^{\eta-2m} - (\epsilon_3 - \epsilon_1)^{\eta-2m} \right) \quad (3-11)$$

where m is determined from a creep test in torsion.

The methods of Soderberg and Bailay differ very little and are in reasonable agreement with experiment. A comparison of the predictions of Eqs. (3-10) and (3-11) has been made by some authors (24) who showed that the difference between them is small and hence the simpler set of Eqs. (3-10) is to be preferred.

3.2.4 Maximum Shear Stress Approach

This approach relates stresses and strain rates in some other manner than by Eq. (3-5) and (3-6). It follows the theory which states that only the maximum shear stress determines the ability of a multiaxial stress system to cause yielding and plastic deformation.

Writing:

$$\begin{aligned}\sigma^{*'} &= \sigma_1 - \sigma_3 \\ \epsilon^{*'} &= \dot{\epsilon}_1 - \dot{\epsilon}_3\end{aligned}\tag{3-12}$$

where $\sigma_1 > \sigma_2 > \sigma_3$, we have, instead Eq (3-8), (13):

$$\begin{aligned}\dot{\epsilon}_1 &= \frac{2 \epsilon^{*'}}{3 \sigma^{*'}} \left(\sigma_1 - 1/2 (\sigma_2 + \sigma_3) \right) \\ \dot{\epsilon}_2 &= \frac{2 \epsilon^{*'}}{3 \sigma^{*'}} \left(\sigma_2 - 1/2 (\sigma_3 + \sigma_1) \right) \\ \dot{\epsilon}_3 &= \frac{2 \epsilon^{*'}}{3 \sigma^{*'}} \left(\sigma_3 - 1/2 (\sigma_1 + \sigma_2) \right)\end{aligned}\tag{3-13}$$

In problems where the other $\sigma_1 > \sigma_2 > \sigma_3$ does not change during the test, Eqs. (3-13) may be easier to handle than Eq. (3-8).

The evidence indicates that the strain rates in steady-state multiaxial stress test correlate better on the basis of the invariant (Soderberg Approach) than by using the maximum shear stress condition.

A comparison of experimental strain rates and predicted strain rates by preceding approaches for biaxial stress state can be seen in the Table 3-1 (25).

3.3 Creep Rates under Biaxial Stress

The effects of combined stress can be seen more clearly by considering biaxial creep with $\sigma_3 = 0$ and $-1 \leq \sigma_2/\sigma_1 \leq 1$ rather than the general case of triaxial stress $\sigma_3 \leq \sigma_2 \leq \sigma_1$. Actually little loss of generality is involved, since a hydrostatic component, which does not influence plastic flow, can be subtracted from a stress state to give $(\sigma_1 - \sigma_3)$, $(\sigma_2 - \sigma_3)$, and 0, as the principal stresses used for calculation of plastic strains (13).

For $\sigma_3 = 0$ in Eqs. (3-10) we obtain :

$$\begin{aligned}\dot{\epsilon}_1 &= B (\sigma_1^2 - \sigma_1 \sigma_2 + \sigma_2^2)^{\frac{n-1}{2}} \left(\sigma_1 - \frac{\sigma_2}{2} \right) \\ \dot{\epsilon}_2 &= B (\sigma_1^2 - \sigma_1 \sigma_2 + \sigma_2^2)^{\frac{n-1}{2}} \left(\sigma_2 - \frac{\sigma_1}{2} \right) \\ \dot{\epsilon}_3 &= B (\sigma_1^2 - \sigma_1 \sigma_2 + \sigma_2^2)^{\frac{n-1}{2}} \left(\frac{-\sigma_1 - \sigma_2}{2} \right)\end{aligned} \quad (3-14)$$

writing the stress ratio $\sigma_2/\sigma_1 = \alpha$ (where $-1 \leq \alpha \leq 1$) and the strain rate produced by the stress σ_1 acting in

tension as $\dot{\epsilon} = B \sigma_1^n$ (Eq. (2-2)), eqs. (3-14) become :

$$\begin{aligned} \frac{\dot{\epsilon}_1}{\dot{\epsilon}} &= (1 - \alpha + \alpha^2)^{\frac{n-1}{2}} \left(1 - \frac{\alpha}{2} \right) \\ \frac{\dot{\epsilon}_2}{\dot{\epsilon}} &= (1 - \alpha + \alpha^2)^{\frac{n-1}{2}} \left(\alpha - \frac{1}{2} \right) \\ \frac{\dot{\epsilon}_3}{\dot{\epsilon}} &= (1 - \alpha + \alpha^2)^{\frac{n-1}{2}} \left(\frac{-1 - \alpha}{2} \right) \end{aligned} \quad (3-15)$$

Examining Eqs. (3-15) we see that largest strain rate (numerically) is $\dot{\epsilon}_1$ for $-1 \leq \alpha \leq 1/2$ while $\dot{\epsilon}_3$ is the largest for $1/2 \leq \alpha \leq 1$. This latter strain rate is negative if σ_1 is a tensile stress. These results follow directly from the assumption of constant volume that is made in obtaining Eq. (3-2).

The large changes in strain rate which may be produced by changes in α , show the importance of estimating correctly the state of multiaxial stress if strain predictions are of importance in the design.

4.1 General Considerations

It is customary to talk about "thin" and "thick" vessels. This distinction refers to the thickness-to-diameter ratio. In a "thin" vessel this ratio is small enough (say less than $1/10$) so that the tangential pressure stress can be taken as constant across the wall thickness.

The stresses in thin-walled vessels produced by internal pressure are found from force balance (equilibrium) considerations only, and hence are true for elasticity, creep, or any kind of material behavior.

In a thin-walled vessel the radial stress, which equals $-p$ (internal pressure) at the inside wall and zero at the outside wall, is small compared with the other two principal stresses and may usually be neglected.

Under creep conditions, it is possible to develop local strain concentrations in the pressure vessels as a result of the constraint imposed by the closure. To close a pressure vessel operating under creep conditions, we should, ideally, avoid strain concentration by matching the creep rates of shell and closure. At the same time, to avoid premature rupture, the maximum tensile stress in the closure should not be excessive.

It is recalled that for a ductile metal under multiaxial stresses at room temperature, it is usually assumed and confirmed by experiment that the shear invariant (Eq. (3-11)) determines the ability of the stress state to produce yielding and subsequent plastic deformation (21). The shear invariant, together with the corresponding quantity involving strains (Eq. (3-1a)), also correlated well with the fracture data for ductile metals at room temperature (21) and, as discussed in Section 3.1, governs the strain rate in multiaxial creep tests. For brittle materials, on the other hand, it is often assumed that the maximum shear stress (Eq. (3-12)) in a multiaxial stress state controls the fracture. However, creep fracture is usually a more complex phenomenon than fracture at room temperature and it depends on other variables such as stress, temperature, composition, heat treatment, and method of manufacture. With these complications in mind we should have reservations about applying any simple criterion, unconfirmed by experiment, to predict rupture under multiaxial stress.

4.2 Thin-walled Vessels under Internal Pressure

4.2.1 Design

4.2.1.1 General Considerations

The type of part being designed will largely determine the basis on which a design stress is chosen (18):

-In steam turbines, small clearances must be maintained throughout a long operating life and design must be on the basis of very small creep rates.

-For high temperature piping, on the other hand, dimensional tolerance is relatively unimportant and the condition to be avoided is rupture within the design life.

-The efficient choice of high-temperature bolting steels requires relaxation test data or their prediction from constant-stress creep data.

-The design stress for slender members carrying a compressive load may have to be based on buckling considerations.

In all cases, except perhaps those in which rupture is the basis of design, the allowable stresses will have to be based on creep data combined to some extent with stress analysis.

When rupture, rather than excessive strain, is the condition to be avoided, the design is faced with the prediction of rupture life under multiaxial stress.

The design stress chosen for a part may depend greatly on the opportunity for inspection and the convenience of replacement or repair if required. The hazards and inconveniences associated with failure must also be evaluated. For example, we may compare the operation of power station with that of an oil refinery or a chemical plant. Periodic shutdowns in refineries and chemical plants usually permit

inspection, and parts showing excessive creep can be removed or repaired. Power-station shutdowns, on the other hand, are usually at less frequent intervals. Furthermore, an interruption of service by failures would be more critical in a public power station than in a private plant. As a result of these considerations, the oil industry uses less conservative stresses than power plants. Potential hazard is also of importance in this connection. It is clear that failure in an oil cracking furnace or superheated steam tube would be a great deal less dangerous than one in an external oil transfer line or main steam pipe, and hence the allowable stresses should be modified accordingly.

The lifetime for which a unit is designed is of obvious importance in choosing allowable stresses and materials. For units with a short design life, a considerable increase in design stress can often be obtained by adequate heat treatment. A similar increase for units with an expected life of, say, 100,000 Hrs. is limited by the uncertainty in predicting material behavior over an extended period.

The design life will also influence the extent to which short-time properties, such as yield strength or tensile strength, are important compared with long-time properties, such as creep or rupture life.

Fluctuating stress and temperature conditions are encountered in many applications (18) (26) (27). For example, the pressure and temperature in a power plant may fluctuate

to suit load requirements or the stress in a furnace tube under constant pressure but will increase if the wall thickness is reduced by corrosion.

There are many other factors to be considered in material selection and choice of design stresses for elevated temperature applications, which may have possible interrelation with creep.

In many cases elevated temperatures introduce the related problem of thermal stresses. In this case, thermal conductivity, short-time tensile strength, thermal-expansion coefficient, surface heat-transfer coefficients, and elastic constants may govern the choice of materials (18) (28) (29) (30).

The resistance of a material to mechanical shock, or impact, must be adequate at the operating temperature and on subsequent cooling (18) (31). This is important for metals which may show embrittlement after extended periods at high temperature.

Three other factors, corrosion and oxidation (18) (32) (33) (34) fatigue and damping capacity (18) (35) (36) (37) (38) and irradiation (18) (39) (40) (41), while important in themselves, may also influence to some extent the creep behavior of a material.

The availability of materials and their cost are important, and there may be cases where economic considerations and availability of creep-resistant materials may dictate

the choice of material and design stresses (42) (43) (44).

In addition to meeting cost requirements and having suitable high-temperature properties, the chosen material must be possible to fabricate by the appropriate forming operations, including welding, if necessary. Generally, the problems of fabrication increase as the material becomes more creep-resistant.

4.2.1.2 Temperatures and Design Stresses

In most applications of steel, creep is not important in design at ambient temperatures, while at sufficiently high temperatures the design may have to be based wholly on creep considerations. For the intermediate range of temperatures the designer must decide on the relative importance of short-time properties (yield point, ultimate strength) and creep properties (rupture life, creep rate).

An analysis of the temperatures and design stresses can thus be based, rather arbitrarily, on three temperature range in which:

- Short-time properties are important.
- Both short-time and creep properties are important
- Creep properties are important.

4.2.1.2 Temperatures at which Short-time Properties are Important and their Design Stresses.

Kerkhof (45) has analyzed the allowable membrane stresses for welded carbon-steel boilers and pressure vessels and has given 575°F as the upper temperature limit for which short-time properties are important. The limit of this range is often taken as 650°F rather than the value of 575°F previously indicated, but Clark (46) has stated that for low-alloy steels this is very conservative and short-time properties predominate in importance well above 650°F. A German Code for Creep Testing of Steel (47) states that the yield point determined in a short-time test gives dependable information on the behavior under static tensile loads only up to about 662°F for plain carbon steels and possibly up to about 842°F for alloy steels.

The ASME "Unfired Pressure Vessel Code" (48) and the ASME "Boiler Code" both specify that below the creep range the allowable stresses are the lowest obtained from:

- 25 per cent of the specified minimum tensile strength at room temperature
- 25 per cent of the minimum expected tensile strength at temperature
- 62 1/2 per cent of the minimum expected yield strength for 0.2 per cent offset, at temperature

The above values apply to the range in which only the short-time properties need be considered. The test results for each specific material help to establish better the upper limit of the temperature range in which only short-time properties are important. For example, in the test realized (46) on a carbon steel (0.15% C), on an 18-8 stainless steel (0.2% offset strain), and on a Mo steel (5% Cr), under the following test conditions:

-Carbon Steel at 600°F and 30,000 psi

-18-8 Stainless steel at 500°F stressed to the yield point

-Mo steel at 800°F and at 1,000°F and 50,000 psi,

the following results were obtained:

The carbon steel elongated to 0.39 per cent but showed no measurable creep rate at 1,000 Hrs.

The 18-8 stainless steel gave a strain of 0.324 per cent after 5 Hrs and no appreciable elongation thereafter.

The Mo steel (at 800°F and 50,000 psi) gave a strain of 0.25 per cent, most of which had occurred in the first few hours and the creep rate was not measurable.

In the Mo steel (at 1,000°F and 50,000 psi), failure occurred in 110 hrs.

As the stresses for all three materials are well above the values given by the "ASME Unfired Pressure Vessel Code", we would conclude that design could be based only on short-

time properties up to at least 600° F for the Carbon Steel and at least 300° F for the other two materials.

These short-time properties, as for example the ultimate tensile strength, must be determined at the design temperature. The foregoing analysis applies to boilers and pressure vessels. In applications involving higher stresses and shorter lives than pressure vessels, it may not be possible to neglect creep properties at the temperatures given above.

4.2.1.4 Temperatures at which Both Short-Time and Creep Properties are Important and Their Design Stresses.

Kerkhof (45) has discussed the allowable membrane stresses for welded carbon-steel boilers and pressure vessels and has found that beyond 575° F to 750° F, the stress-strain curve for carbon steel shows no real yield point, and hence, both short-time and creep properties are important.

The intermediate range in which both elastic and plastic properties are important is more difficult to define. The "ASME Unfired Pressure Vessel Code", specifies that:

- In the transition range of temperatures, the stress allowances were limited to values obtained from a smooth curve, joining the values for the low and high temperature ranges, the curve lying on or

below the curve of 62 1/2 per cent of the minimum expected yield strength at temperature.

4.2.1.5 Temperatures at Which Creep Properties Are Important and Their Design Stresses.

Herchof (45) has discussed the allowable membrane stresses for welded carbon steel boilers and pressure vessels and has found that above 750° F complete relaxation of secondary stresses will occur in a short-time, and design can be based on creep properties.

The "ASME Unfired Pressure Vessel Code" for the upper range of temperatures, at which only creep properties need be considered, specifies that:

-At high temperatures, the stress values are based on 100 per cent of the stress to produce a creep rate of 1/100 per 1,000 hours; the values so chosen being based on a conservative average of many reported tests as evaluated by the subcommittee; greater weight being given to longer time tests in evaluating data. In addition to the above-stated creep strength requirements, stress values were also limited to 100% of the stress to produce rupture at the end of 100,000 hours; the values so chosen being based on a conservative average as evaluated by the subcommittee.

The "ASME Boiler Code" allows the same stress base on creep strain but only 60 per cent of the average, or 80 per cent of the minimum stress to cause rupture in 100,000 hours. As the creep-stress limit is usually considerably lower than for rupture, the two codes often lead to the same design values.

The choice of the above values does not necessarily mean that the vessel will show 1 per cent of strain or rupture in 100,000 hours. Service temperatures and pressures are usually less than design values; wall thicknesses are often increased by corrosion allowance, and material properties are usually above those specified, all of which results in an increased factor of safety.

To illustrate some of the preceding analysis, the change in tensile strength, yield strength, rupture strength and creep strength with the temperature and the ASME code allowable stress for a 5 Cr-0.5% Mo steel are drawn in Fig. 4-1 (18) from the data given by Clark (46). It is interesting to note the decrease in the allowable stress given by the code which take place above the temperature at which long-time and short-time properties coincide.

The code requirements apply to vessels and boilers with an expected life of at least 100,000 hours. The general method might also be applied to the design of a unit intended for a shorter life of, say, 1,000 hours.

In the low-temperature range the elastic stresses are

based on short-time properties with an appropriate safety factor.

The stresses in the upper temperature range are based on long-time properties (permissible strain or rupture in 100,000 hours).

In the intermediate-temperature range the stresses are obtained by drawing a smooth curve between the high and low temperature values.

The type of application will, of course, influence the choice of a safety factor in the low-temperature range and the extent to which creep strain or rupture is important.

4.2.2 Design Conditions

4.2.2.1 Design Criterion

It is assumed that the operating temperatures are in the upper range of temperatures, at which only creep properties need be considered, and hence, design has to be based wholly on creep considerations.

Design must be based on the maximum permissible creep rates, and thus the stresses are based on the permissible strain or rupture life in 100,000 hours.

It is considered that constant-stress tension-creep data are available for the temperature at which we wish to make the stress analysis and that the data have been extra-

olated, if necessary, to the time duration of interest. Unless otherwise stated, the temperature is taken as constant.

4.2.2.2 Creep Type

It is assumed that the creep curves from test data show a well defined region of steady-state creep, and that this latter contributes most of the strain; hence, design may be based on only steady-state creep.

As we have seen, small changes in such variables as stress, temperature, composition, heat treatment, or method of manufacture may greatly influence creep behavior, and hence a simple empirical expression for creep data may be adequate for rational design.

4.2.2.3 Approach

We use the Soderberg Approach based on Mises invariant (Eqs. (3-5) and (3-6)), which is accurate only when steady-state creep predominate. The methods of Soderberg and Bailly differ very little and are in reasonable agreement with experiment. However the Soderberg approach is to be preferred because it has simpler equations.

The evidence also indicates that the strain rates in steady-state multiaxial stress tests correlate better on the

basis of lines invariant than by using the maximum shear stress approach.

4.2.2.4 Stress State

In a thin-walled vessel the radial stress (σ_3), which equals $-p$ (internal pressure) at the inside wall and zero at the outside wall, is small compared with the other two principal stresses and may usually be neglected. Hence, we have the case of a thin-walled vessel under a biaxial stress state.

Under creep conditions, the relationship between stress and strain rate is generally nonlinear, and hence the stresses must be considered as a combined effect, rather than separately, which greatly complicates a creep analysis. In some cases the stress analysis is simple while in other cases it may form the main problem of creep analysis.

The effect of biaxial stresses can be seen more clearly by considering biaxial creep with $\sigma_3 = 0$ and $1 \leq \sigma_2/\sigma_1 \leq 1$ rather than the general case of triaxial stress $\sigma_3 \leq \sigma_2 \leq \sigma_1$. Hence, the creep rates under biaxial stress states may be governed by Eqs. (3-15).

5. RESULTS

Table 5-1 shows the results obtained of the analysis realized in the preceding sections.

The curves of Fig. 5-1 were plotted from the data shown in the table 5-1. These curves may be used for the design of thin-walled vessels under internal pressure and with the consideration of steady-state creep.

...
(2) ...
...
...

- Yield changes in the stress ratio $\sigma_2/\sigma_1 = \alpha$
may ...

- The largest strain rate (numerically) is $\dot{\epsilon}_1$
for $-1 \leq \alpha \leq 1/2$ while $\dot{\epsilon}_3$ is the
largest for $1/2 \leq \alpha \leq 1$.

- As n increases, the effect of small errors
in stress becomes increasingly important.

- The value of n may be obtained from creep
test data for the temperature at which we
wish to make the stress analysis or from
the extrapolate creep test data.

7. CONCLUSIONS

According to the analysis of results (Table 5-1 and Fig. 5-1 of the preceding section, we reach the following conclusions:

- The large changes in strain rate which may be produced by small changes in the stress ratio ($\sigma_2 / \sigma_1 = \alpha$) show the importance of correctly estimating the state of multiaxial stress if design is based on strain predictions.
- The effect of small errors in the stress become increasingly important, as n increases which shows the importance of estimating correctly the values of n from creep data or from the extrapolated creep data.
- The curves of Fig. 5-1 may be used for design purpose of thin-walled vessels under internal pressure and consideration of steady-state creep.

NOTATION

P	Load
ϵ	Unit Strain
t	Time
ϵ_0	Instantaneous Strain (or initial creep strain)
$\dot{\epsilon}$ or $d\epsilon/dt$	Strain Rate
t_r	Rupture Life or Rupture Time
E	Efficiency
T, T_1, T_2	Absolute Temperature
ϵ_c	Creep Strain
$\dot{\epsilon}_c$	Creep Rate
σ_0	Constant Initial Stress
σ	Stress
ΔH	Activation Energy
R	Gas Constant
$\sigma_1, \sigma_2, \sigma_3$	Principal Stresses
$\epsilon_1, \epsilon_2, \epsilon_3$	Creep Strains
$\dot{\epsilon}_1, \dot{\epsilon}_2, \dot{\epsilon}_3$	Creep Strain rates
σ^*	Stress in Multiaxial Stress state
$\dot{\epsilon}^*$	Strain rates in terms of σ^*
ϵ^*	Strain in terms of σ^*

2. LIST OF TABLES

Table 3-1

Comparison of Principal Creep Strain by Different Approaches with Biaxial Stress Creep experiments.

Best data of Tapsell and Johnson (25) for 0.17 per cent carbon steel at 850° F.

Table 5-1:

Strain Ratios as a Function of Stress Ratios for thin-walled Vessels under Internal Pressure and Conditions of Steady-State Creep.

Table 3-1. Comparison of Principal Creep Strain by Different Approaches with Biaxial Stress Creep Experiments. Test data of Tappell and Johnsons (25) for 0.17 per cent carbon steel at 850 F. Strain rates given are $\text{Hr}^{-1} \times 10^6$

Stress, psi	Experimental			Soderberg Approach			Bailey Approach			Max. Shear stress Approach		
	ϵ_1	ϵ_2	ϵ_3	ϵ_1	ϵ_2	ϵ_3	ϵ_1	ϵ_2	ϵ_3	ϵ_1	ϵ_2	ϵ_3
14,660	0.99	-0.80	-0.19	0.95	-0.49	-0.46	0.96	-0.50	-0.46	1.00	-0.50	-0.47
12,350	0.72	-0.57	-0.15	0.68	-0.35	-0.33	0.68	-0.36	-0.32	0.67	-0.35	-0.32
12,080	2,080	1.04	0.37	-1.41	0.76	-0.45	-0.31	0.77	-0.48	-0.29	0.80	-0.49
14,980	2,580	1.76	-0.24	-1.52	1.22	-0.73	-0.49	1.17	-0.72	-0.45	1.28	-0.79
9,720	3,720	0.75	-0.21	-0.54	0.59	-0.42	-0.17	0.60	-0.44	-0.16	0.66	-0.49
8,100	3,100	0.47	0.15	-0.62	0.39	-0.28	-0.11	0.40	-0.30	-0.10	0.44	-0.11
7,530	4,470	0.52	-0.30	-0.22	0.42	-0.35	-0.07	0.43	-0.36	-0.07	0.49	-0.41
10,240	6,240	1.09	-1.13	0.04	0.84	-0.70	-0.14	0.86	-0.73	-0.13	0.97	-0.83
5,900	5,900	0.34	-0.34	0	0.36	-0.36	0	0.37	-0.37	0	0.43	-0.43
7,720	7,720	0.68	-0.58	0	0.66	-0.66	0	0.68	-0.68	0	0.78	-0.78

Table 5-1. Strain Ratios in Function of Stress Ratios for Thin-Walled Vessels under Internal Pressure and Conditions of Steady-State Creep.

STRAIN RATIO	ALPHA *	AN *	STRA #	AN	STRA	AN	STRA	AN	STRA	AN	STRA	AN	STRA	AN	STRA
ε ₁ /ε ₂	-1.0	1.0000	1.5000	3.7988	6.9787	4.0000	7.7942	6.0000	7.7942	8.0000	7.7942	8.0000	7.7942	12.0000	1.3325
ε ₂ /ε ₃	-1.0	1.0000	1.5000	3.7988	6.9787	4.0000	7.7942	6.0000	7.7942	8.0000	7.7942	8.0000	7.7942	12.0000	1.3325
ε ₁ /ε ₃	-1.0	1.0000	1.5000	3.7988	6.9787	4.0000	7.7942	6.0000	7.7942	8.0000	7.7942	8.0000	7.7942	12.0000	1.3325
ε ₂ /ε ₁	0.8	1.0000	1.3000	3.7988	4.5296	4.0000	4.9548	4.0000	4.9548	4.0000	4.9548	4.0000	4.9548	12.0000	0.1351
ε ₃ /ε ₁	0.6	1.0000	1.1000	3.7988	3.3337	4.0000	3.5672	4.0000	3.5672	4.0000	3.5672	4.0000	3.5672	12.0000	0.5096
ε ₂ /ε ₂	0.6	1.0000	1.1000	3.7988	3.3337	4.0000	3.5672	4.0000	3.5672	4.0000	3.5672	4.0000	3.5672	12.0000	0.5096
ε ₃ /ε ₂	0.6	1.0000	1.1000	3.7988	3.3337	4.0000	3.5672	4.0000	3.5672	4.0000	3.5672	4.0000	3.5672	12.0000	0.5096
ε ₁ /ε ₁	0.4	1.0000	1.2000	3.7988	2.5129	4.0000	2.3381	4.0000	2.3381	4.0000	2.3381	4.0000	2.3381	12.0000	0.5452
ε ₂ /ε ₁	0.4	1.0000	1.2000	3.7988	2.5129	4.0000	2.3381	4.0000	2.3381	4.0000	2.3381	4.0000	2.3381	12.0000	0.5452
ε ₃ /ε ₁	0.4	1.0000	1.2000	3.7988	2.5129	4.0000	2.3381	4.0000	2.3381	4.0000	2.3381	4.0000	2.3381	12.0000	0.5452
ε ₁ /ε ₁	0.2	1.0000	1.7000	3.7988	1.4865	4.0000	1.5189	4.0000	1.5189	4.0000	1.5189	4.0000	1.5189	12.0000	0.0991
ε ₂ /ε ₁	0.2	1.0000	1.7000	3.7988	1.4865	4.0000	1.5189	4.0000	1.5189	4.0000	1.5189	4.0000	1.5189	12.0000	0.0991
ε ₃ /ε ₁	0.2	1.0000	1.7000	3.7988	1.4865	4.0000	1.5189	4.0000	1.5189	4.0000	1.5189	4.0000	1.5189	12.0000	0.0991
ε ₁ /ε ₁	0.0	1.0000	1.0000	3.7988	1.9459	4.0000	1.9663	4.0000	1.9663	4.0000	1.9663	4.0000	1.9663	12.0000	0.3855
ε ₂ /ε ₁	0.0	1.0000	1.0000	3.7988	1.9459	4.0000	1.9663	4.0000	1.9663	4.0000	1.9663	4.0000	1.9663	12.0000	0.3855
ε ₃ /ε ₁	0.0	1.0000	1.0000	3.7988	1.9459	4.0000	1.9663	4.0000	1.9663	4.0000	1.9663	4.0000	1.9663	12.0000	0.3855
ε ₁ /ε ₁	0.0	1.0000	1.5000	3.7988	1.5000	4.0000	1.5000	4.0000	1.5000	4.0000	1.5000	4.0000	1.5000	12.0000	1.0000
ε ₂ /ε ₁	0.0	1.0000	1.5000	3.7988	1.5000	4.0000	1.5000	4.0000	1.5000	4.0000	1.5000	4.0000	1.5000	12.0000	1.0000
ε ₃ /ε ₁	0.0	1.0000	1.5000	3.7988	1.5000	4.0000	1.5000	4.0000	1.5000	4.0000	1.5000	4.0000	1.5000	12.0000	1.0000
ε ₁ /ε ₁	0.2	1.0000	1.3000	3.7988	2.7051	4.0000	2.3310	4.0000	2.3310	4.0000	2.3310	4.0000	2.3310	12.0000	0.5050
ε ₂ /ε ₁	0.2	1.0000	1.3000	3.7988	2.7051	4.0000	2.3310	4.0000	2.3310	4.0000	2.3310	4.0000	2.3310	12.0000	0.5050
ε ₃ /ε ₁	0.2	1.0000	1.3000	3.7988	2.7051	4.0000	2.3310	4.0000	2.3310	4.0000	2.3310	4.0000	2.3310	12.0000	0.5050
ε ₁ /ε ₁	0.4	1.0000	1.6000	3.7988	4.449	4.0000	4.638	4.0000	4.638	4.0000	4.638	4.0000	4.638	12.0000	0.1768
ε ₂ /ε ₁	0.4	1.0000	1.6000	3.7988	4.449	4.0000	4.638	4.0000	4.638	4.0000	4.638	4.0000	4.638	12.0000	0.1768
ε ₃ /ε ₁	0.4	1.0000	1.6000	3.7988	4.449	4.0000	4.638	4.0000	4.638	4.0000	4.638	4.0000	4.638	12.0000	0.1768
ε ₁ /ε ₁	0.6	1.0000	1.8000	3.7988	5.449	4.0000	5.300	4.0000	5.300	4.0000	5.300	4.0000	5.300	12.0000	0.1550
ε ₂ /ε ₁	0.6	1.0000	1.8000	3.7988	5.449	4.0000	5.300	4.0000	5.300	4.0000	5.300	4.0000	5.300	12.0000	0.1550
ε ₃ /ε ₁	0.6	1.0000	1.8000	3.7988	5.449	4.0000	5.300	4.0000	5.300	4.0000	5.300	4.0000	5.300	12.0000	0.1550
ε ₁ /ε ₁	0.8	1.0000	2.0000	3.7988	6.4701	4.0000	6.2319	4.0000	6.2319	4.0000	6.2319	4.0000	6.2319	12.0000	0.1150
ε ₂ /ε ₁	0.8	1.0000	2.0000	3.7988	6.4701	4.0000	6.2319	4.0000	6.2319	4.0000	6.2319	4.0000	6.2319	12.0000	0.1150
ε ₃ /ε ₁	0.8	1.0000	2.0000	3.7988	6.4701	4.0000	6.2319	4.0000	6.2319	4.0000	6.2319	4.0000	6.2319	12.0000	0.1150
ε ₁ /ε ₁	1.0	1.0000	1.0000	3.7988	5.0000	4.0000	5.0000	4.0000	5.0000	4.0000	5.0000	4.0000	5.0000	12.0000	0.5000
ε ₂ /ε ₁	1.0	1.0000	1.0000	3.7988	5.0000	4.0000	5.0000	4.0000	5.0000	4.0000	5.0000	4.0000	5.0000	12.0000	0.5000
ε ₃ /ε ₁	1.0	1.0000	1.0000	3.7988	5.0000	4.0000	5.0000	4.0000	5.0000	4.0000	5.0000	4.0000	5.0000	12.0000	0.5000

* AT PPA : Stress Ratios ($\sigma_2/\sigma_1 = \infty$)

AN : Constant n from Eq. (2-2) ($\epsilon_c = B \sigma^n$)

STRA : Strain Ratios from Eqs. (3-15)

1. APPENDIX FIGURES

- Fig. 1-1: Schematic Creep Curve
- Fig. 1-2: Schematic Relaxation Curve
- Fig. 2-1: Relaxation curves: (a) Carbon steel (at 500°F, initial stress 10,000 psi); (b) Tread rubber (at 130°C, initial elongation 50 per cent)
- Fig. 2-2: Typical tensile stress-rupture data: (a) Asphalt (pitch-type bitumen); (b) Killed carbon steel (Timken Roller Bearing Co); (c) Reinforced Plastic (polyester fiberglass laminate)
- Fig. 3-1: Schematic creep curves two stresses: (A) and (B), method of idealizing as steady-state creep only. (C) and (D), as steady state plus lumped transient creep.
- Fig. 3-2: Creep curve showing initial elastic and plastic strains as well as transient creep.

Fig. 4-1

Change of the different stress values with temperature and the ASME code allowable stresses for 5 Cr-10 steel

Fig. 5-1

Strain Ratios as a Function of Stress Ratios for Thin-Walled Vessels under Internal Pressure and Conditions of Steady-State Creep.

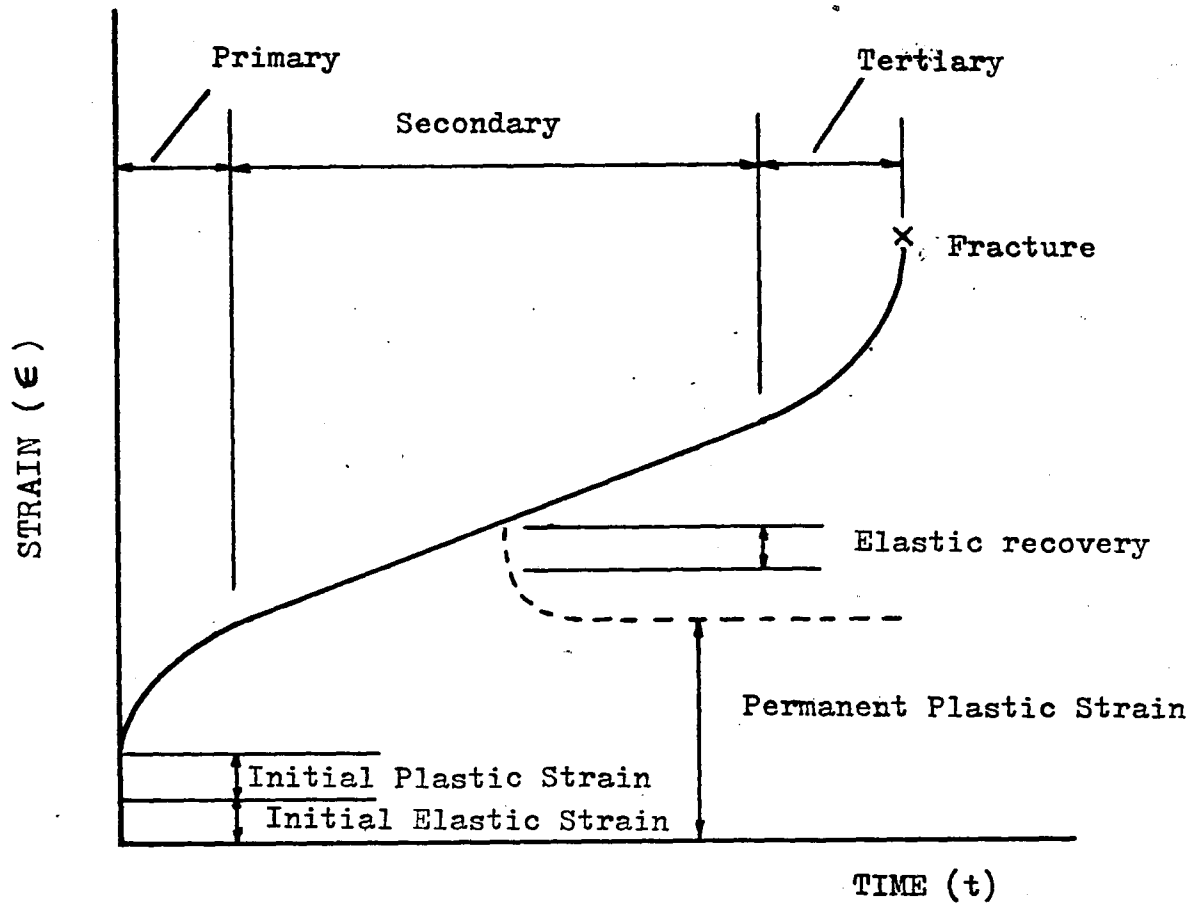


Figure 1-1. Schematic creep curve. Dashed line shows behavior on unloading.

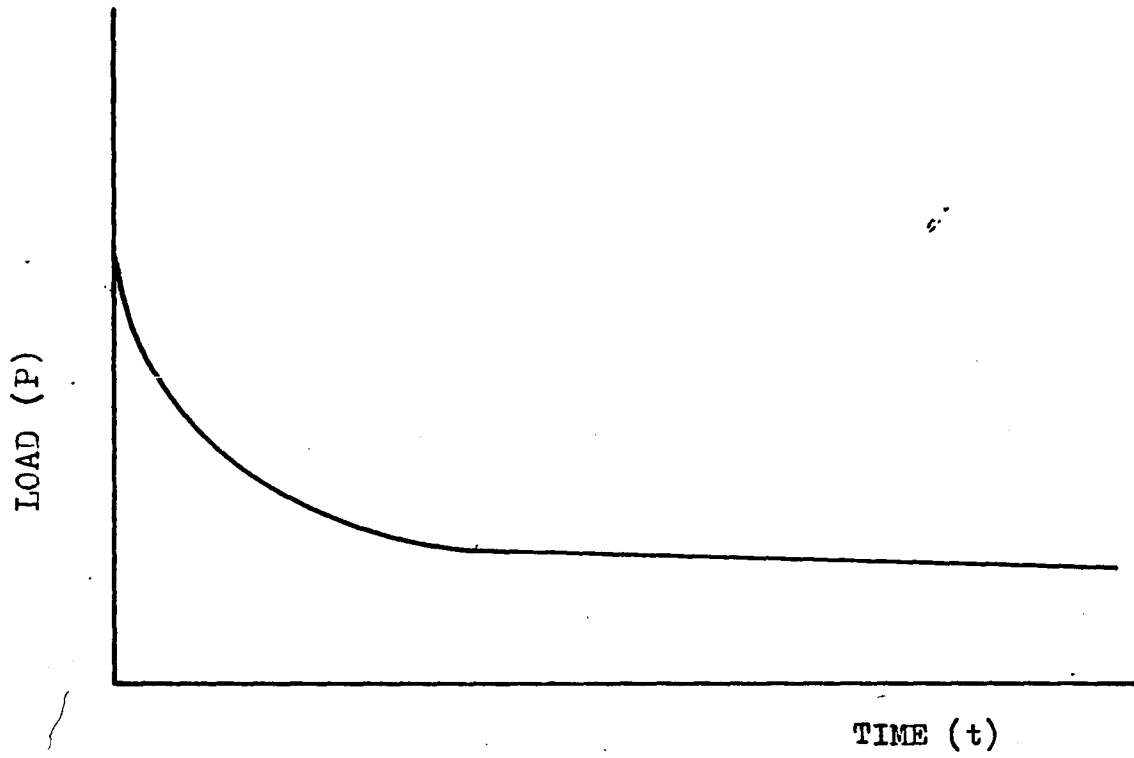


Figure 1-2. Schematic relaxation curve.

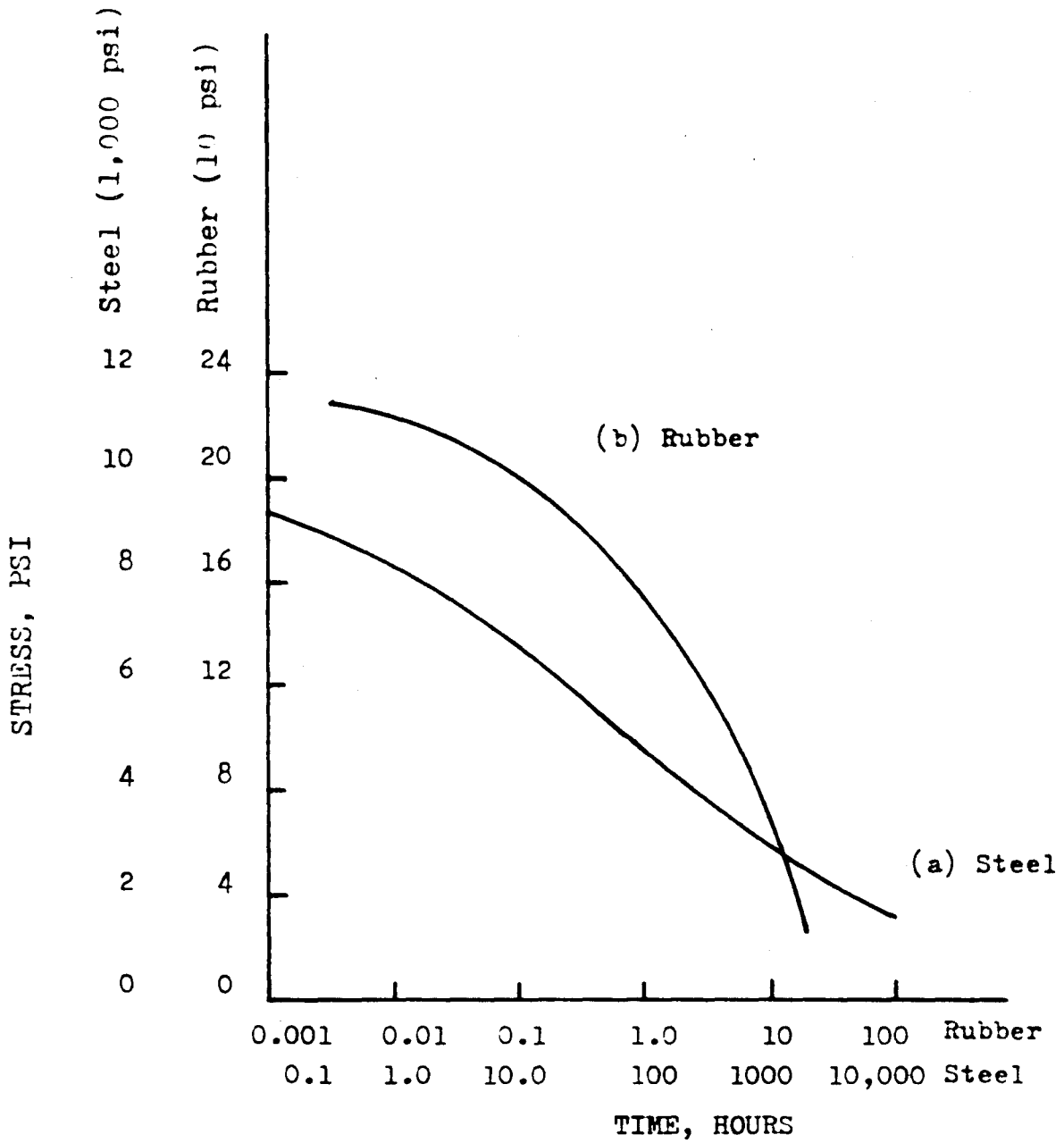


Figure 2-1. Relaxation curves: (a) Carbon Steel (at 850 F, initial stress 10,000 psi); (b) Tread rubber (at 130 C, initial elongation 50 per cent)

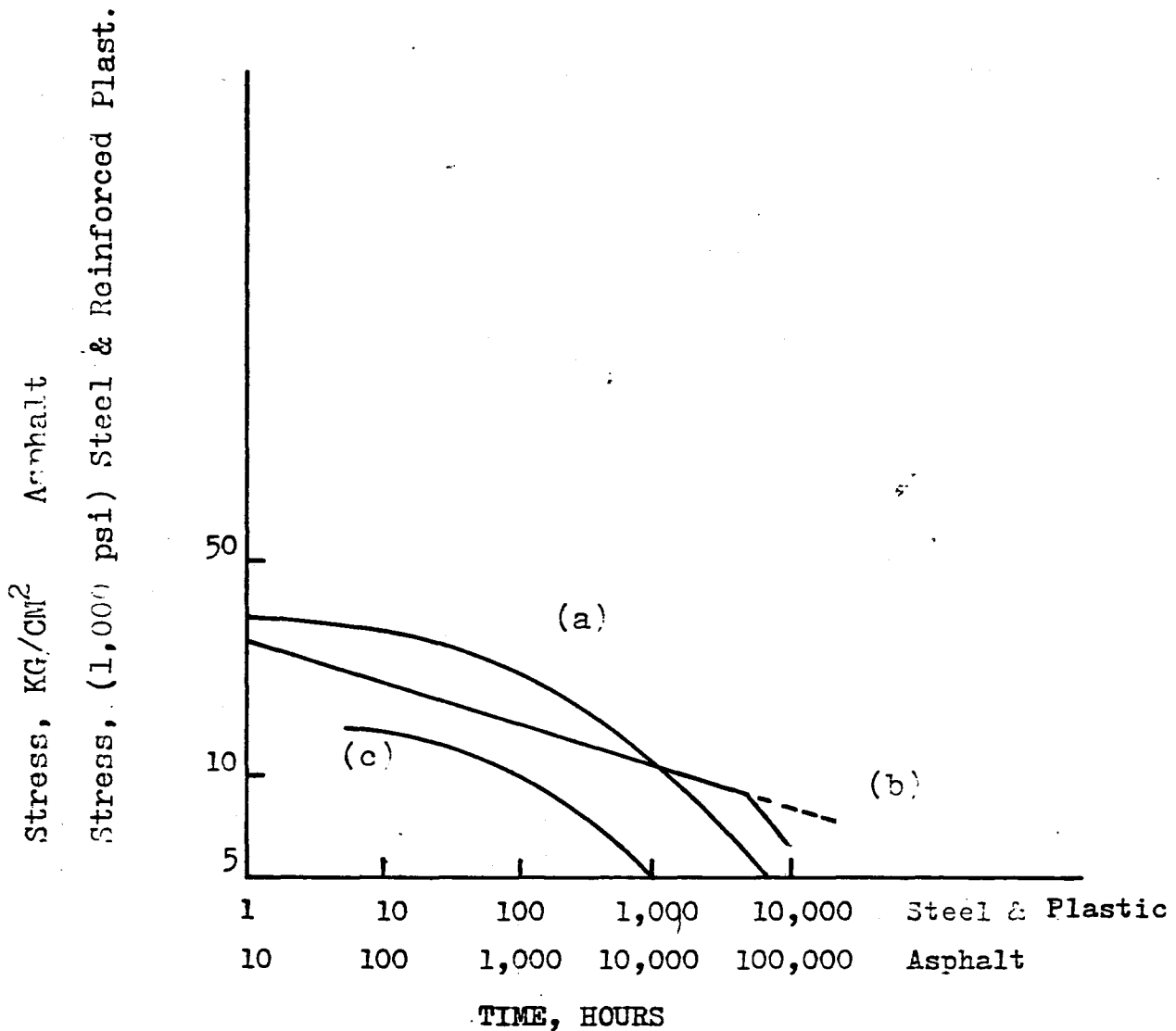


Figure 2-2. Typical tensile stress-rupture data:
 (a) Asphalt (pitch-type bitumen); (b) killed carbon steel (Timken Roller Bearing Co); (c) Reinforced plastic (polyester fiberglass laminate)

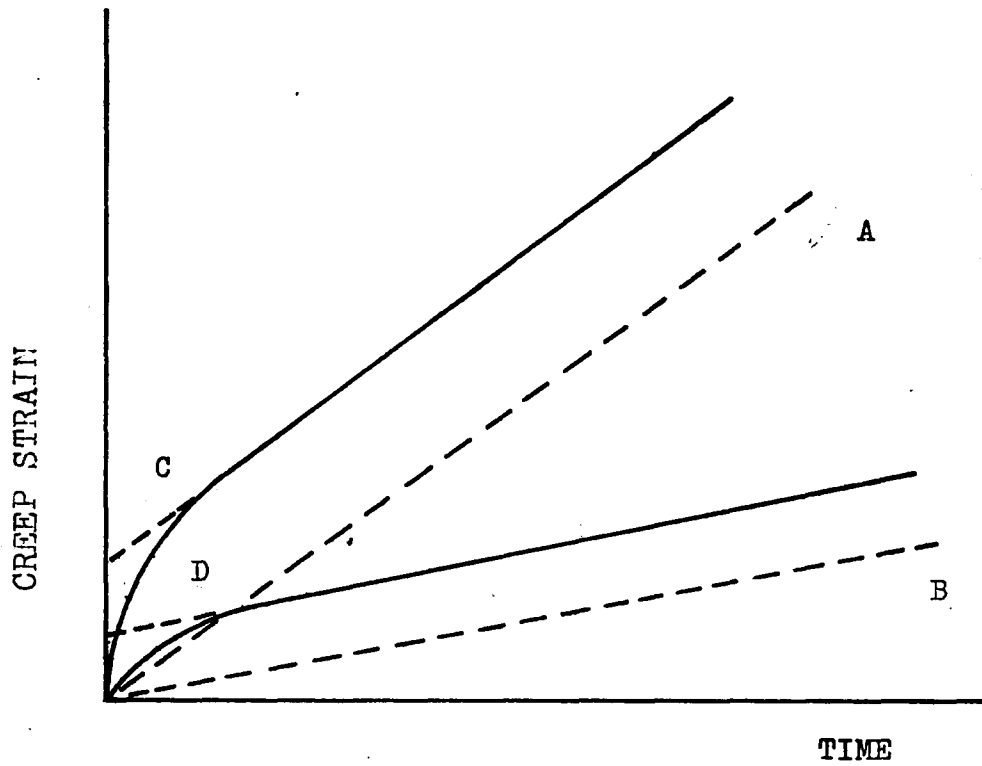


Figure 3-1. Schematic creep curves for two stresses: (A) and (B), method of idealizin as steady-state. (C) and (D), as steady state plus lumped Transient creep.

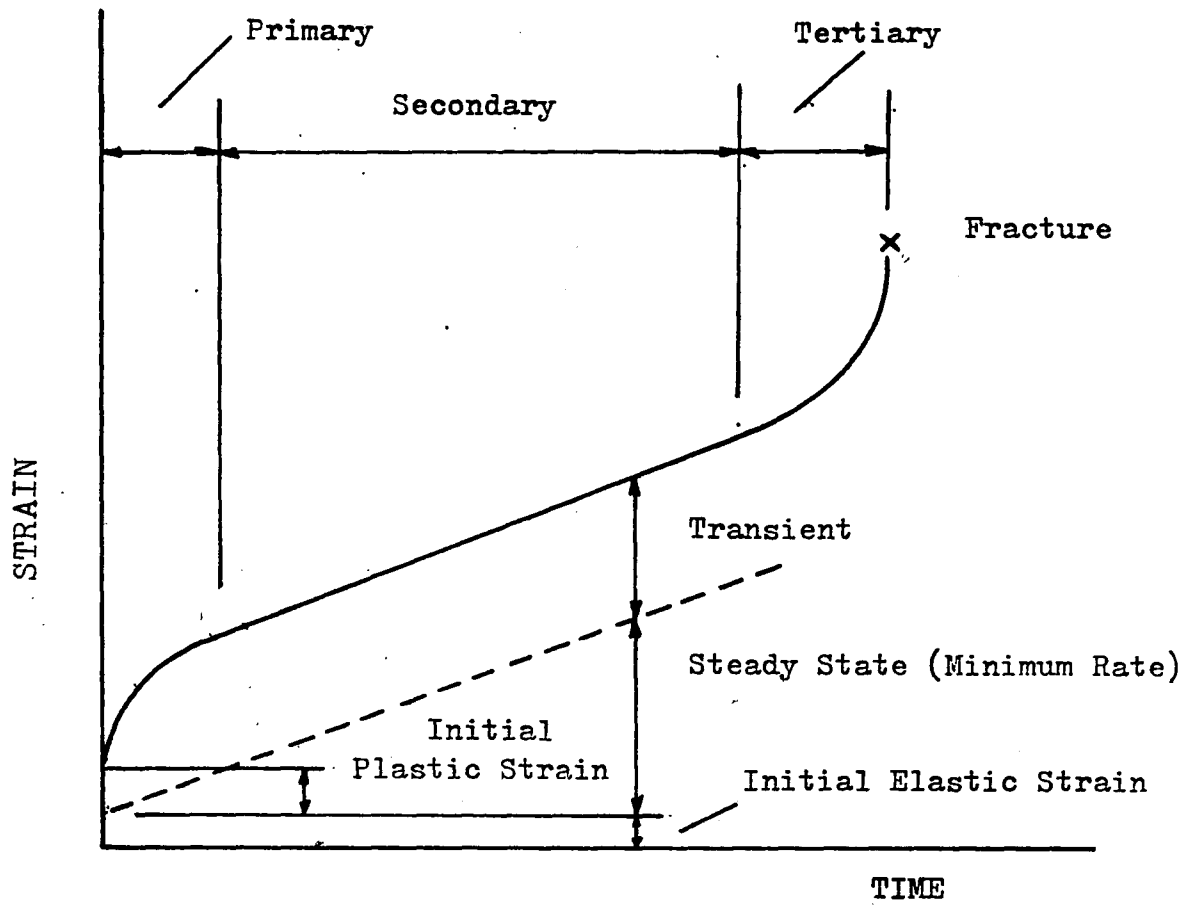


Figure 3-2. Creep curve showing initial elastic and plastic strains as well as transient creep.

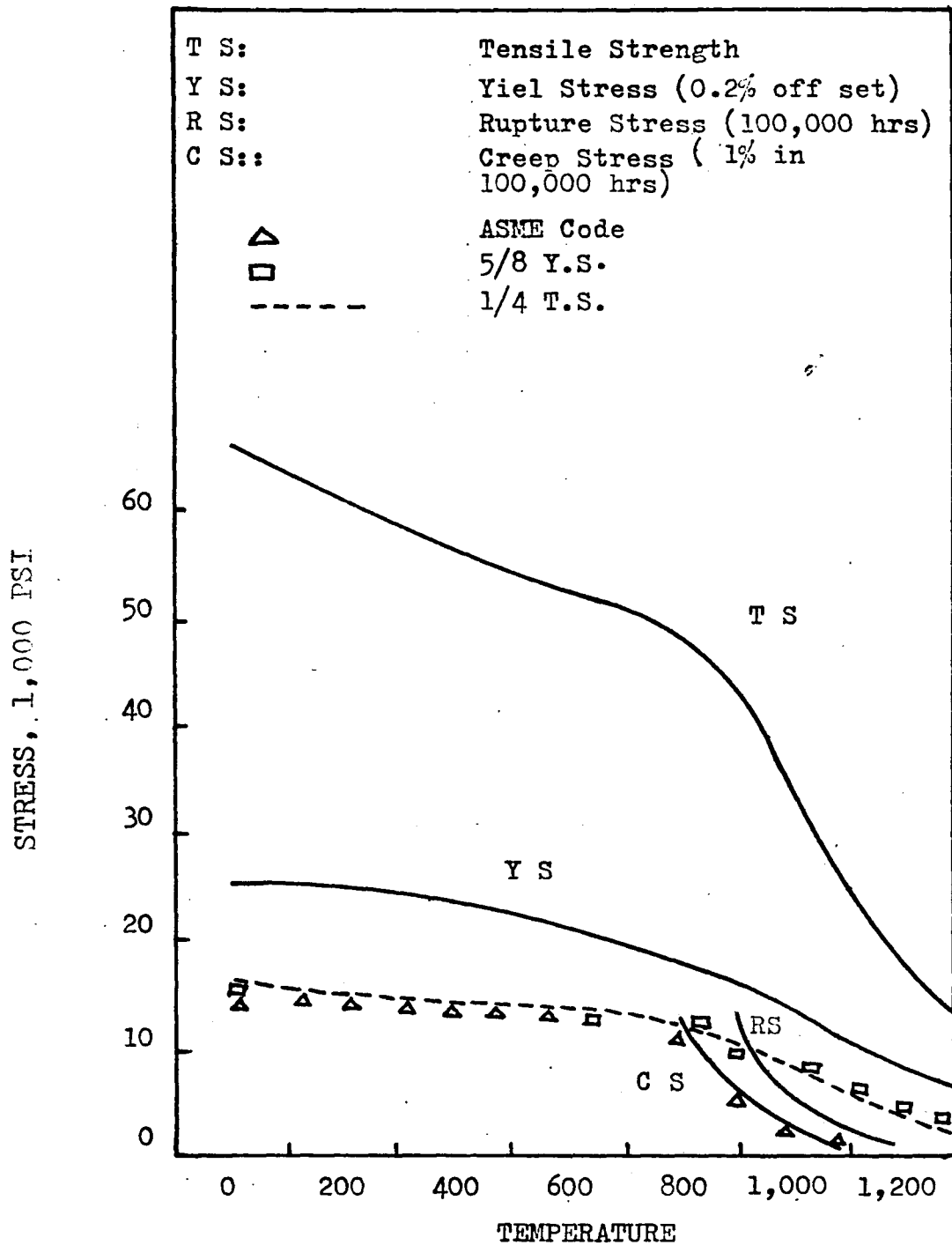


Figure 4-1. Change of the different stress values with temperature and the ASME code allowable stresses for 5 Cr-0.5 M steel

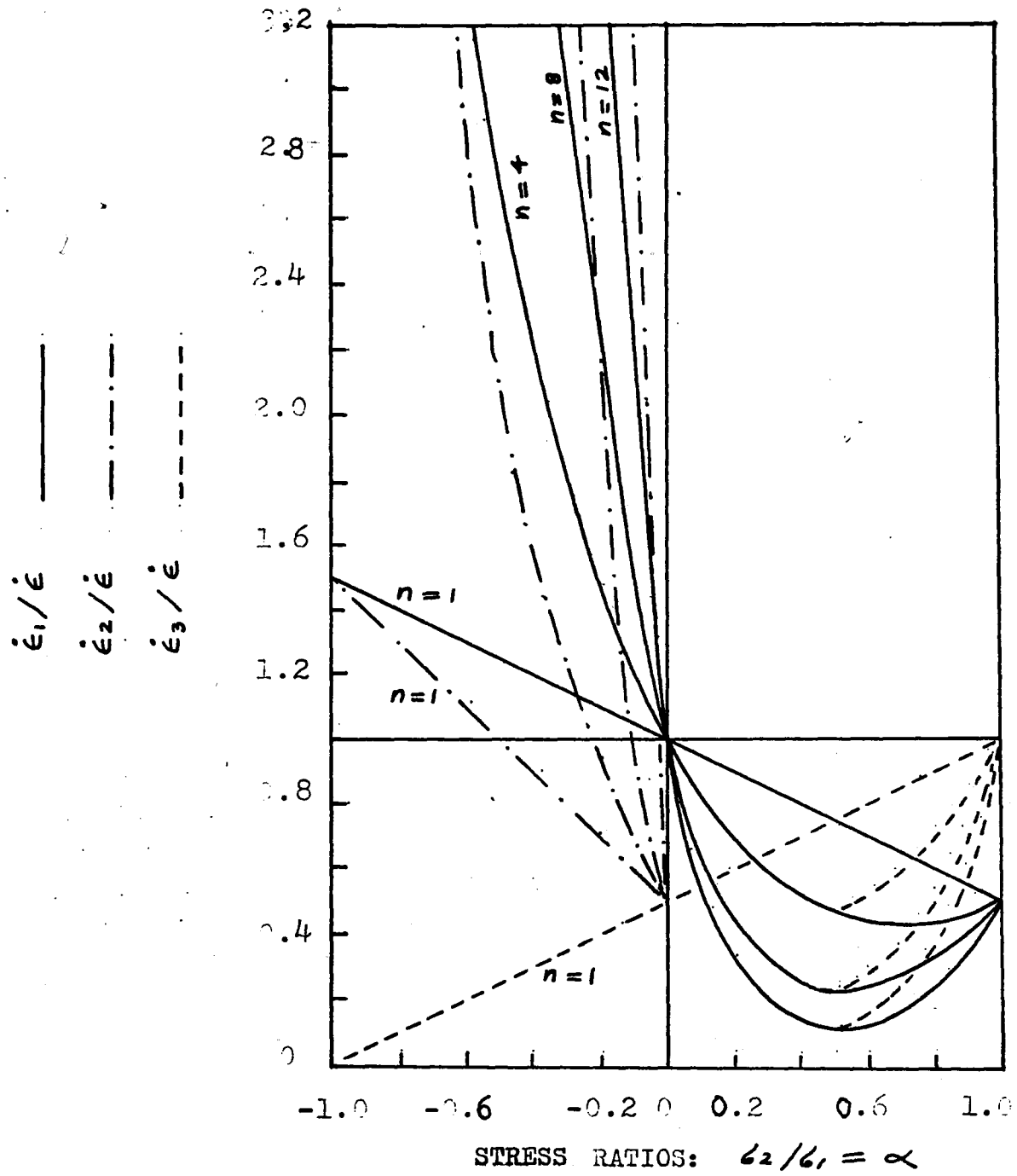


Figure 5-1. Strain Ratios in Function of Stress Ratios for Thin-Walled Vessels under Internal Pressure and Conditions of Steady-State Creep.

II. LIST OF REFERENCES

1. GURRY, A.N., "Metallic Creep and Creep Resistant Alloys", Chapt. 4, Butterworth & Co. Ltd., London, 1949.
2. HANMER, S.J., "Interpretation and Use of Creep Results", J. Am. Soc. Metals 24: 57A, 1952.
3. STEINER, C.J.F., de BERBADILLO, J.J., PENSE, A.J., and STOUT, R.D., "The Creep Rupture Properties of Pressure Vessels", Welding Journal Research Supplement, April 1962.
4. WATTE, O.H., "Transient Creep in Pure Metals", Proc. Phys. Soc., London, B66: 549, 1953.
5. COOPER, A.H., "The Time Laws of Creep", J. Mech. and Phys. Solids, 1:53, 1952.
6. JOHNSON, A.E., and FROST, H.J., "The Temperature dependence of Transient and Secondary Creep of an aluminum Alloy to British Standard 2142 at temperatures between 20° and 250° C and Constant Stress", J. Inst. Metals, 51: 93, 1952-1953.
7. HAZLETT, T.H., and PARKER, E.R. "Nature of the Creep Curve", J. Metals, 51: 93, 1952-1953.

8. FASSON, J., "On a New Representation Resembles the Maxwell", Rev. Met., 36: 171, 1933.
9. VETTER, E.G., "Creep of Metals at Elevated Temperatures--The Hyperbolic Sine Relation between Stress and Creep Rate", Trans. ASME, 65: 761, 1943.
10. CORN, J.E., "Some Fundamental Experiments on High Temperature Creep", National Physical Laboratory Symposium on Creep and Fracture of Metals at High Temperature, Teddington, England, H. M. Stationary Office, London, p. 89, 1956.
11. WEBERMAN, J., and SHAMIRAN, A., "Creep of Polycrystalline Nickel", J. Metals, 8:1223, 1956.
12. SERVI, F.S., and GRANT, H.J., "Creep and Stress rupture of Aluminum as a Function of Purity", J. Metals, 3:939, 1951.
13. ROBERT, L., "Prediction of Relaxation of Metals from Creep Data", Proc. ASTM, 51, 111, 1951.
14. TOBOLSKY, A.V., and ANDREWS, R.D., "Systems manifesting Superposed Elastic and Viscous Behavior", J. Chem. Phys., 13:3, 1945.

15. VAN DER BOEK, G., "Building Materials, Their elasticity, North-Holland Publishing Company, Amsterdam, The Netherlands, 1954.
16. "Digest of Steel for Elevated Temperature Service", 5th ed., Whinton Roller Bearing Company, Canton, Ohio, 1946.
17. SCHNEIDER, G., "Time-Temperature Relationships for Rupture Stresses in Reinforced Plastic", Proc. ASTM, 54: 1344, 1954.
18. TURNER, I., and HELLER, A.R., "Creep of Engineering materials", Mc Graw-Hill, New York, 1959.
19. MORRISON, P.H., "Creep in Tubular Pressure Vessels", Trans. ASME, 61: 239, 1939.
20. BAILEY, R.E., "The Utilization of Creep Test Data in Engineering Design", Proc. Inst. Mech. Engrs., 131: 131, 1935.
21. NADAI, A., "Theory of Flow and Fracture of Solids", McGraw-Hill, New York, 1950.
22. JOHNSON, A.E., "Creep under Complex Stress Systems at Elevated Temperatures", Proc. Inst. Mech. Engrs., 164: 432, 1951.

20. COOPERBERG, C.R., "Interpretation of Creep Tests for Machine Design", trans. ASME, 57: 733, 1936.
24. MAAMI, J., "Mechanical Properties of Material properties of Materials and Design", Chap. 6, MacGraw-Hill, New York, 1942.
25. BALSWELL, H.J., and JOHNSON, A.E., "Creep under Combined Tension and Torsion", Engineering, 151: 24, 1946.
26. ROBINSON, E.L., "Effect of Temperature Variation on the Creep Strength of Steel", Trans. ASME, 61: 253, 1939.
27. ROBINSON, E.L., "Effect of Temperature Variation on the Long Time Rupture Strength on Steels", trans. ASME, 74:777, 1952.
28. Symposium on Effect of Cyclic Heating and Stressing of Metals at Elevated Temperatures, ASTM Spec. Tech. Publ. 165, 1954.
29. CHINE, C.H., "Resistance to Thermal Shock", J. Am. Rocket Soc., 21:147, 1951.
30. DIMENSION, H., "Thermal Fatigue and Thermal Shock", Welding Research Council Bull. Ser. 10, April, 1952.
31. SHIRAH, G.V., "Properties of Metals at Elevated Temperatures", McGraw-Hill, New York, 1950.

... ..
... ..
... ..
... ..

Um

... ..
... ..
... ..

64. "The effect of", *J. Chem. Phys.*, **19**, 1951.

65. "The effect of", *J. Chem. Phys.*, **19**, 1951.

66. "The effect of", *J. Chem. Phys.*, **19**, 1951.

67. "The effect of", *J. Chem. Phys.*, **19**, 1951.

68. "The effect of", *J. Chem. Phys.*, **19**, 1951.

1. WHEEL, G.C., and HUNNINGER, G.C., "Effect of Nuclear Irradiation", J. Metals, 7: 411, 1954.
2. Wren, G.L., "Low Alloy Steels for Automotive Turbines", AIAA Annual Meeting, Detroit, Mich., Jan. 9, 1954.
3. CASMAN, J.F., SHANNON, G.A., and FASHNER, G.J., "High Nitrogen Austenitic Cr-Ni Steels", Trans. Am. Soc. Metals, 47:53, 1955.
4. SHANNON, G.A. and FASHNER, G., "Development on High Temperature Steels and Alloys for Gas Turbines", Iron Steel Inst. Trans. Part. 43, 1952, p. 219.
5. HUNNINGER, G.C., "Allowable Membrane Stresses for Welded Carbon Steel Boilers and Pressure Vessels", ASME Paper 51-104. -1.
6. SHANNON, G.A., "High Temperature Alloys" Pitman Publishing Corporation, New York, 1953.
7. German Tentative Code for Creep Testing of Steel, DIN Tentative Standard A 117-117, Stahl u. Eisen, 55:1505, 1935. See also Dutch translation 146.
8. Rules for Construction of Unfired Pressure Vessels, "ASME Boiler and Pressure Vessels Code", See viii, ASME, New York, 1954.

49. HARTMAN, Arthur, "Stress, Free Vibration, and Stability Analysis of Thin, Elastic Shells of Revolution", AFWAL-TR-6-104, 119:5, Michigan University, 1967
50. "Correlation of Available High-Temperature Creep characteristics of Metals and Alloys", AIAA and ASEE, 196:126, New York, 1967.
51. ASEE Boiler and Pressure Vessel Code, Division 1, Section VIII, appendix B, ASEE, New York, 1967.

12. GENERAL DESIGN DATA

12.1 Specifications and Working Conditions

According to the flow diagram of the installation, the working conditions of the pressure vessel are the following:

- Fluid: superheat vapor
- Temperature: 752° F (400° C)
- Pressure: 50 psia (3.5 kg/cm²)
- Subjected to abnormal temperature excursions of up to 1,112° F (600° C). Total duration of the excursions during lifetime, about 100 hours.

Specifications of the vessels (Fig. 12-1 and 12-2) are the following:

Shell

Cylindrical surface:

- Inside diameter 315.96 in
(808 cm)
- Length 314.96 in
(800 cm)
- Thickness of internal refractory 4in (10.6 cm)

Closure

Spherical Surface:

- Radius (R) 29.37 in
(750 cm)
- Angle (ϕ) 150°
- Thickness of material refractory 4 in (10.2 cm)

Toroidal surface:

- Radius (R) 275.59 in
(7000 cm)
- Angle (ϕ) 30°
- Thickness of internal refractory 4 in (10.2 cm)

12.2 Design Criterion

In the design the worst conditions are considered during the abnormal operation of the installation.

According to Section 4.2.1.5 the vessel temperature T ($1,112^\circ\text{F}$) is in the upper range of temperature ($T > 750^\circ\text{F}$) at which only creep properties need be considered, and hence, the design has to be based wholly on creep conditions.

Dimensional tolerance is relatively unimportant and the condition to be avoided is rupture within the design life; thus the design stresses are based on the rupture life of the vessel (Sections 4.2.1.1 and 4.2.2.1).

According to Fig. 12-3, the creep curve from test data of the material shows a well-defined region of steady-state creep, and this region contributes most of the strain. Hence, design may be based on only steady-state creep.

According to Section 4.2.2.4, the pressure vessel is under a biaxial stress state, and creep rates are governed by the eq. (3-15), Section 3.3.

12.3 Stress Calculation

According to Section 7 where the importance of estimating correctly the state of multiaxial stress is shown, we use the Computer Program Dr. Arturs Kalnins (Table 12-1) for the membrane stress calculation for the shell cylindrical surface) and for the closure (spherical and toroidal surface) of vessel (Fig. (12-1) and Fig. (12-2)) (49).

12.4 Material

We choose a material for the vessel with the following specifications (50):

Chemical Composition (%)

C:	0.10
Mn:	0.45
Si:	0.18

C:	0.15
P:	0.17
Cr:	5.09
Mo:	0.55
Heat Treatment	Annealed 1,550° F
Grain Size	7
Brinell Hardness	128
Type of Furnace	Electrical Furnace

Physical Properties at 1,112° F

Tensile Strength	34,000 psi
Yield Stress (0.2% ret)	15,000 psi
Proportional Limit	5,500 psi
Elongation in 2 inches	38.85%
Reduction of Area	83%
Charpy Impact Resistance	
1 hour at temperature	54 Ft-lb
1,000 hour at temperature	55 Ft-lb
Young's modulus	24.5 x 10 ⁶ psi

Creep Properties (46)

Rupture Strength at 1,112° F:

Fracture at 1,000 hours	11,250 psi
Rupture at 10,000 hours	8,750 psi
Rupture at 100,000 hours	6,250 psi

Creep Strength at 1,112° F:

1% at 10,000 hours	5,500 psi
1% at 100,000 hours	3,000 psi

We assume in the design that the material has 1 ⁵/₃₂ inches (2 cm) of thickness, and ³/₃₂ inches (.2 cm) of corrosion allowance.

12.5 Results

The output of the Computer Program (Table 12-1) shows the membrane stress values for the Shell and closure of the vessel.

In the calculation of stresses σ_1 and σ_2 the membrane stresses σ_θ and σ_ϕ , respectively, are only included. The stresses produced by the bending moment ($\sigma_{M\theta}/h^2$ and $\sigma_{M\phi}/h^2$) are included in design rules, according to ASME Boiler and Pressure Vessel Code, Section VIII, Page 9, 1968.

The curves of Figs. (12-4), 12-5) and 12-6) were plotted from the data shown in Table 12-1 and the critical values for the stress ratio of the vessel are the following:

$$\text{Cylindrical surface: } \alpha_{cr} = \frac{\sigma_2}{\sigma_1} = \frac{3,212}{7,727} = 0.4689$$

$$\text{Toroidal surface: } \alpha_{cr} = \frac{\sigma_2}{\sigma_1} = \frac{4,152}{-12.674} = -0.3280$$

$$\text{Spherical Surface: } \alpha_{cr} = \frac{\sigma_2}{\sigma_1} = \frac{5,586}{6,563} = 0.8969$$

We can see from Section 12.3 that strain rate produced by stress σ , acting in tension is:

$$\dot{\epsilon} = B \sigma^n \quad (12-1)$$

Where B and n are constants; both depend upon temperature.

We can determine the values of the constants by using creep properties of the material (Section 12-4):

-At 1,112°F, 1% strain rate in 10,000 hours is produced by a stress of 5,500 psi.

-At 1,112°F, 1% strain rate in 100,000 hours is produced by a stress of 3,000 psi.

Hence, from the Eq. (12-1)

$$\frac{0.01}{10,000} = B \times 5,500^n$$

$$\frac{0.01}{100,000} = B \times 3,000^n$$

$$\text{Then, } 10 = \left(\frac{5,500}{3,000} \right)^n$$

$$n = \frac{\ln 10}{\ln (5,500/3,000)}$$

$$= \frac{2.302585}{0.606136}$$

$$= 3.798793$$

$$\text{and, } \frac{1}{1} = 0.798793$$

$$B = \frac{10^{-6}}{1.6175719} = 6.1821 \times 10^{-21} \frac{\text{in}^{-1}}{\text{psi}}$$

From Fig. 5-1, Section 7, (Curves Plotted From Eqs. 9-15) the strain ratios of the vessel are the following:

<u>Cylindrical Surface</u>		($\alpha_{cr} = 1.4619$)
$\frac{\dot{\epsilon}_1}{\dot{\epsilon}} = 0.5123$	$\frac{\dot{\epsilon}_2}{\dot{\epsilon}} = -0.7205$	$\frac{\dot{\epsilon}_3}{\dot{\epsilon}} = -0.4919$ (12-1a)

<u>Meridional Surface</u>		($\alpha_{cr} = -0.3271$)
$\frac{\dot{\epsilon}_1}{\dot{\epsilon}} = -1.9387$	$\frac{\dot{\epsilon}_2}{\dot{\epsilon}} = 1.3733$	$\frac{\dot{\epsilon}_3}{\dot{\epsilon}} = -0.5573$ (12-1b)

<u>Spherical Surface</u>		($\alpha_{cr} = 0.3969$)
$\frac{\dot{\epsilon}_1}{\dot{\epsilon}} = 0.4315$	$\frac{\dot{\epsilon}_2}{\dot{\epsilon}} = 0.3465$	$\frac{\dot{\epsilon}_3}{\dot{\epsilon}} = -0.3200$ (12-1c)

Replacing the Eq. (12-1) into Eqs. (12-1a), (12-1b), and (12-1c), we can determine the strain rates of the vessel:

<u>Cylindrical Surface</u>	($\sigma_1 = 7,707$ psi in tension)
$\dot{\epsilon}_1 = 0.5123 \times 6.1821 \times 10^{-21} \times 7,707^{2.798793} = \frac{10.4738 \times 10^{-7}}{\text{Hr}}$	

$$\dot{\epsilon}_2 = -0.207 \times 6.1121 \times 10^{-21} \times 7,777^3 \cdot 79,799 = \frac{-7.60 \times 10^{-6}}{\text{hr.}}$$

$$\dot{\epsilon}_3 = -0.4019 \times 6.1121 \times 10^{-21} \times 7,777^3 \cdot 79,799 = \frac{-17.72 \times 10^{-6}}{\text{hr.}}$$

Spherical Surface

($\sigma_1 = 12,674$ psi in tension):

$$\dot{\epsilon}_1 = -1.9337 \times 6.1121 \times 10^{-21} \times 12,674^3 \cdot 79,799 = \frac{-46.1275 \times 10^{-6}}{\text{hr.}}$$

$$\dot{\epsilon}_2 = 1.2719 \times 6.1121 \times 10^{-21} \times 12,674^3 \cdot 79,799 = \frac{22.7362 \times 10^{-6}}{\text{hr.}}$$

$$\dot{\epsilon}_3 = -0.5573 \times 6.1121 \times 10^{-21} \times 12,674^3 \cdot 79,799 = \frac{-13.2345 \times 10^{-6}}{\text{hr.}}$$

Spherical Surface

($\sigma_1 = 6,563$ psi in tension)

$$\dot{\epsilon}_1 = 0.4015 \times 6.1121 \times 10^{-21} \times 6,563^3 \cdot 79,799 = \frac{9.42 \times 10^{-7}}{\text{hr.}}$$

$$\dot{\epsilon}_2 = 0.2465 \times 6.1121 \times 10^{-21} \times 6,563^3 \cdot 79,799 = \frac{6.772 \times 10^{-7}}{\text{hr.}}$$

$$\dot{\epsilon}_3 = -0.3238 \times 6.1121 \times 10^{-21} \times 6,563^3 \cdot 79,799 = \frac{-16.241 \times 10^{-7}}{\text{hr.}}$$

Total strains of the vessel are the following:

Cylindrical Surface:

$$\epsilon_1 = \frac{10.4733 \times 10^{-7} \times 100 \text{ Hr}}{\text{Hr.}}$$

$$= 0.0104733\% \text{ in 100 Hr}$$

$$\epsilon_2 = \frac{-1.7524 \times 10^{-7} \times 100 \text{ Hr}}{\text{Hr.}}$$

$$= -0.0007524\% \text{ in 100 Hr}$$

$$\epsilon_3 = \frac{-17.7275 \times 10^{-7} \times 100 \text{ Hr}}{\text{Hr}}$$

$$= -0.0177275 \text{ in } 100 \text{ Hrs}$$

Toroidal Surface:

$$\epsilon_1 = \frac{-46.3275 \times 10^{-6} \times 100 \text{ Hr}}{\text{Hr}}$$

$$= -0.463275 \text{ in } 100 \text{ Hrs}$$

$$\epsilon_2 = \frac{32.7362 \times 10^{-6} \times 100 \text{ Hr}}{\text{Hr}}$$

$$= 0.327362 \text{ in } 100 \text{ Hrs}$$

$$\epsilon_3 = \frac{-13.2845 \times 10^{-6} \times 100 \text{ Hr}}{\text{Hr}}$$

$$= -0.132845 \text{ in } 100 \text{ Hrs}$$

Spherical Surface:

$$\epsilon_1 = \frac{9.42 \times 10^{-7} \times 100 \text{ Hr}}{\text{Hr}}$$

$$= 0.000942 \text{ in } 100 \text{ Hrs}$$

$$\epsilon_2 = \frac{6.779 \times 10^{-7} \times 100 \text{ Hr}}{\text{Hr}}$$

$$= 0.0006779 \text{ in } 100 \text{ Hrs}$$

$$\epsilon_3 = \frac{-16.281 \times 10^{-7} \times 100 \text{ Hr}}{\text{Hr}}$$

$$= -0.016281 \text{ in } 100 \text{ Hrs}$$

We can compare critical stress and critical strains of the vessel with the ASME code allowable values:

Cylindrical Surface

At 1,112° F, 0.1147 strain (ϵ_1) in
100 hrs is produced by a stress of
7,777 psi

Active

At 1,112° F, ($\epsilon > 0.11$ in 100 hrs),
rupture life in 100 hrs is produced
by a stress of 13,500 psi

Code A-1 Allowable

Spherical Surface

At 1,112° F, 0.2270 strain (ϵ_2)
in 100 hrs is produced by a
stress of 12,674 psi

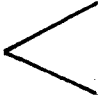
Active

At 1,112° F, ($\epsilon > 0.11$ in 100 hrs),
rupture life in 100 hrs is produced
by a stress of 13,500 psi

Code A-1 Allowable

Spherical Surface

At 1,112°F, 0.0042" strain (ϵ_1)
in 100 Hrs is produced by a stress
of 6,568 psi



At 1,112°F, ($\epsilon > 0.1$ in 100 Hrs),
rupture life in 100 Hrs is produced
by a stress of 13,500 psi

Active

Code ASME Allowable

At 752°F (400°C), the design of the vessel could be based only on short-time properties (46) (49). In this case we can also compare critical stresses of the vessel in normal operation (752°F) with the ASME code allowable values (51):

Cylindrical Surface

7,707 psi at 752°F

12,942 psi at 752°F

Active

Code ASME Allowable

Cylindrical Surface

12,674 psi at 752° F

12,943 psi at 752° F

Spherical Surface

6,562 psi at 752° F

12,943 psi at 752° F

Conclusion

On the basis of the foregoing results, we can use the following material for the pressure vessel:

- | | |
|----------------------|-----------------------------|
| -Specifications | 4-6 Cr Ni Steel (Section 4) |
| -Thickness | 1 5/32 inches (3 cm) |
| -Corrosion Allowance | 3/32 inches (0.2 cm) |

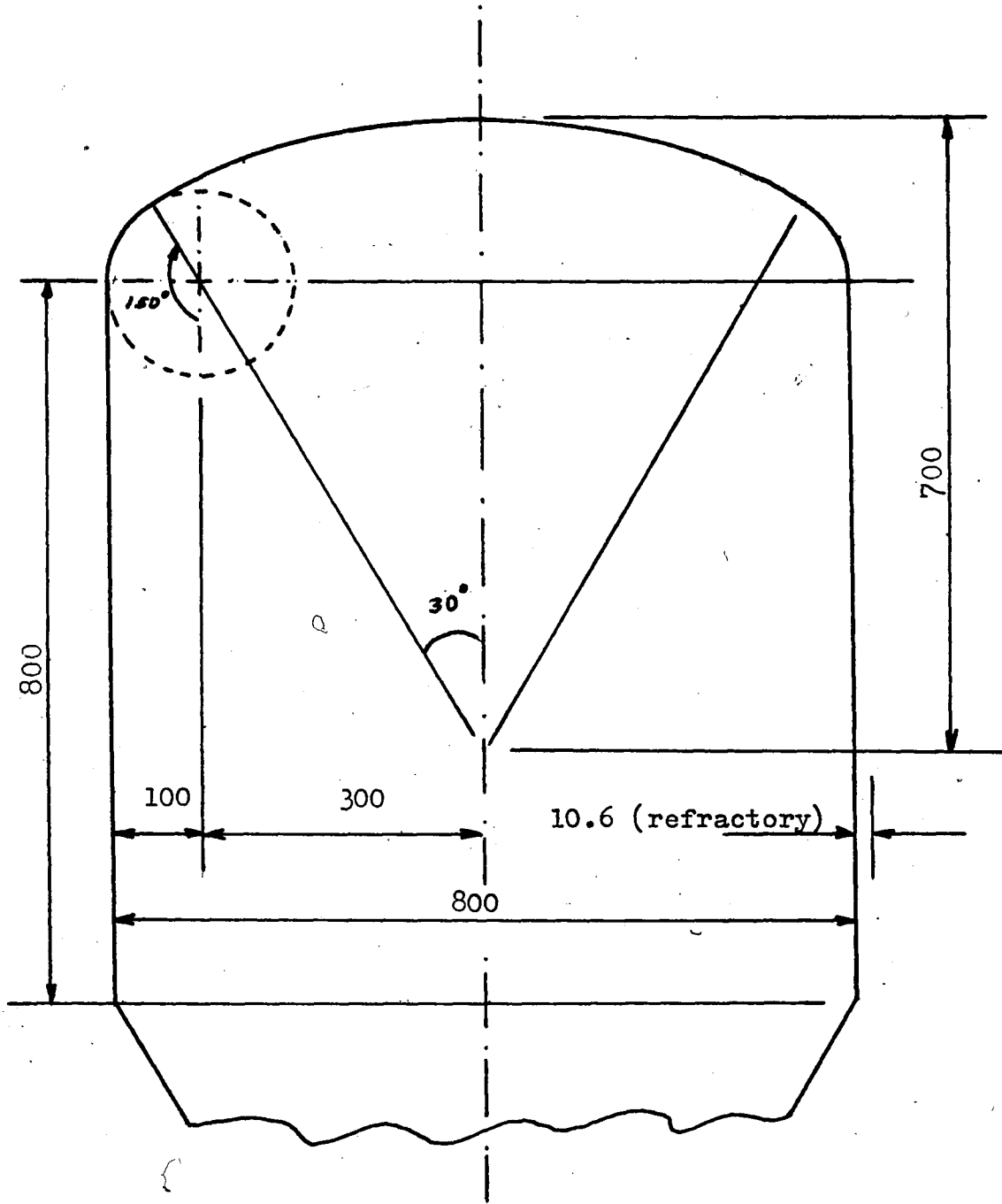


Figure 12.1. Dimension of Pressure Vessel

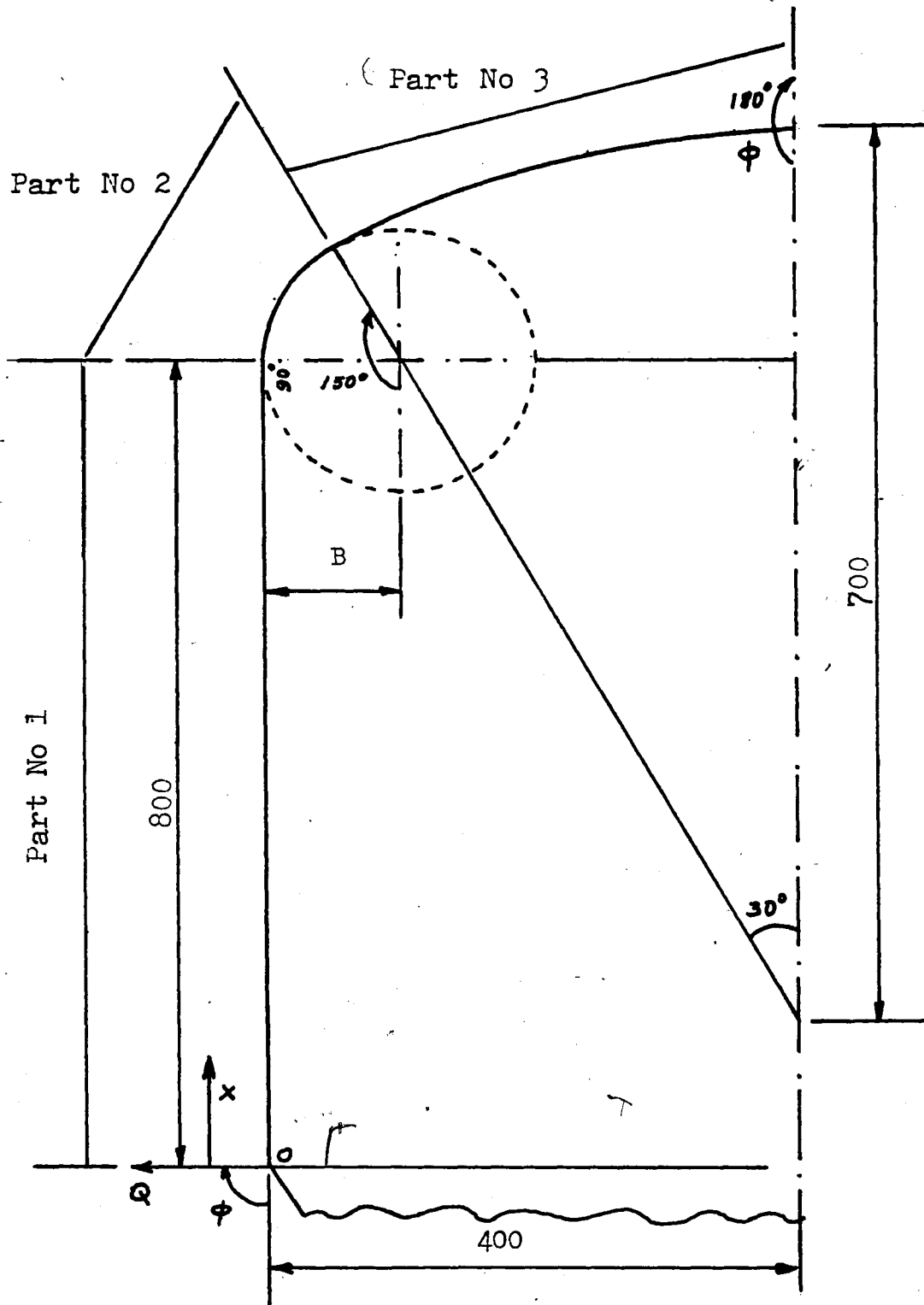


Figure 12-2. Cylindrical Surface (Part No 1)
 Toroidal Surface (Part No 2), and Spherical
 Surface (Part No 3)

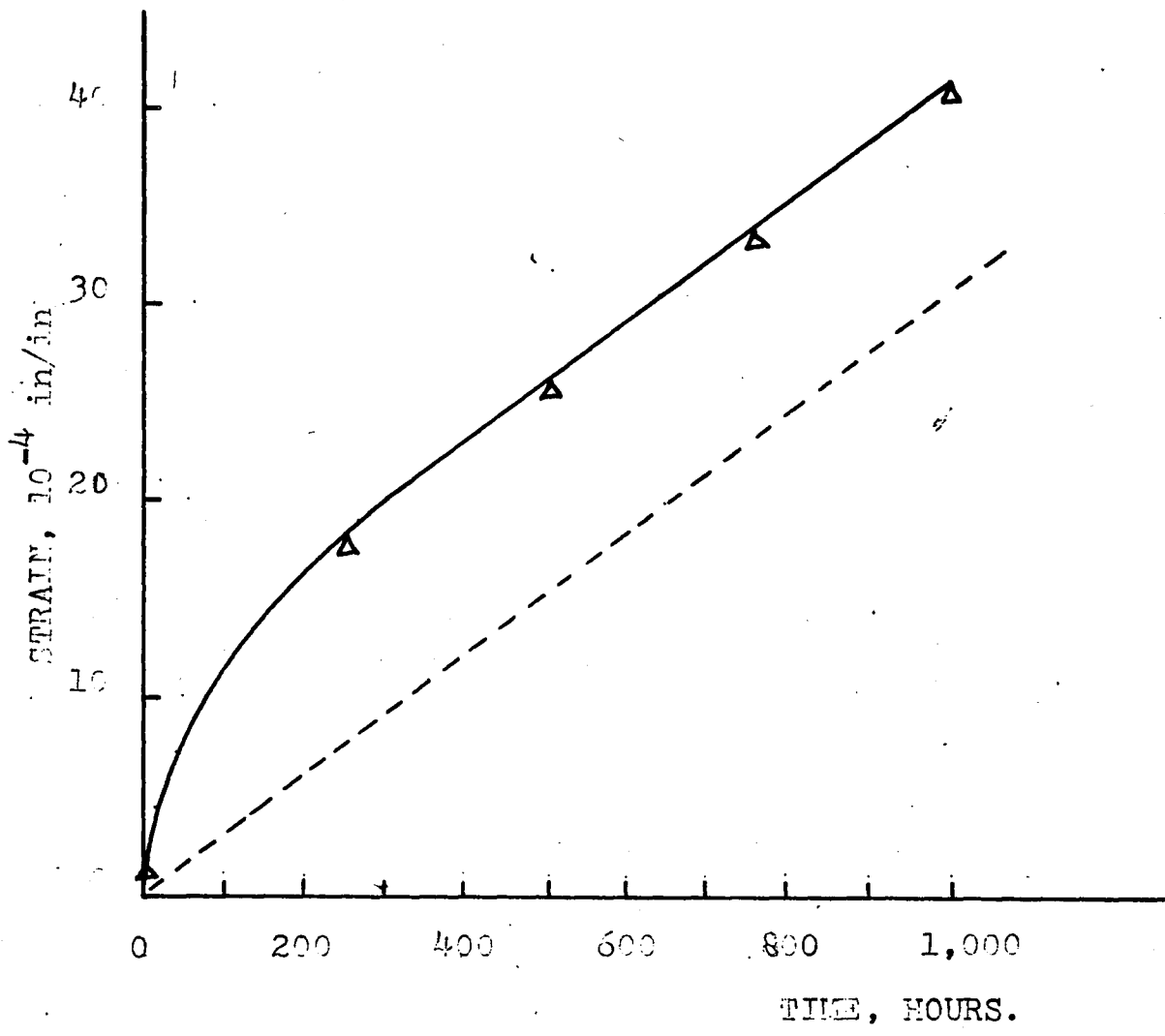


Figure 12-3. Creep curve from test data of 4-Cr M Steel (Testing conditions: 1,100 F, 8,000 psi)

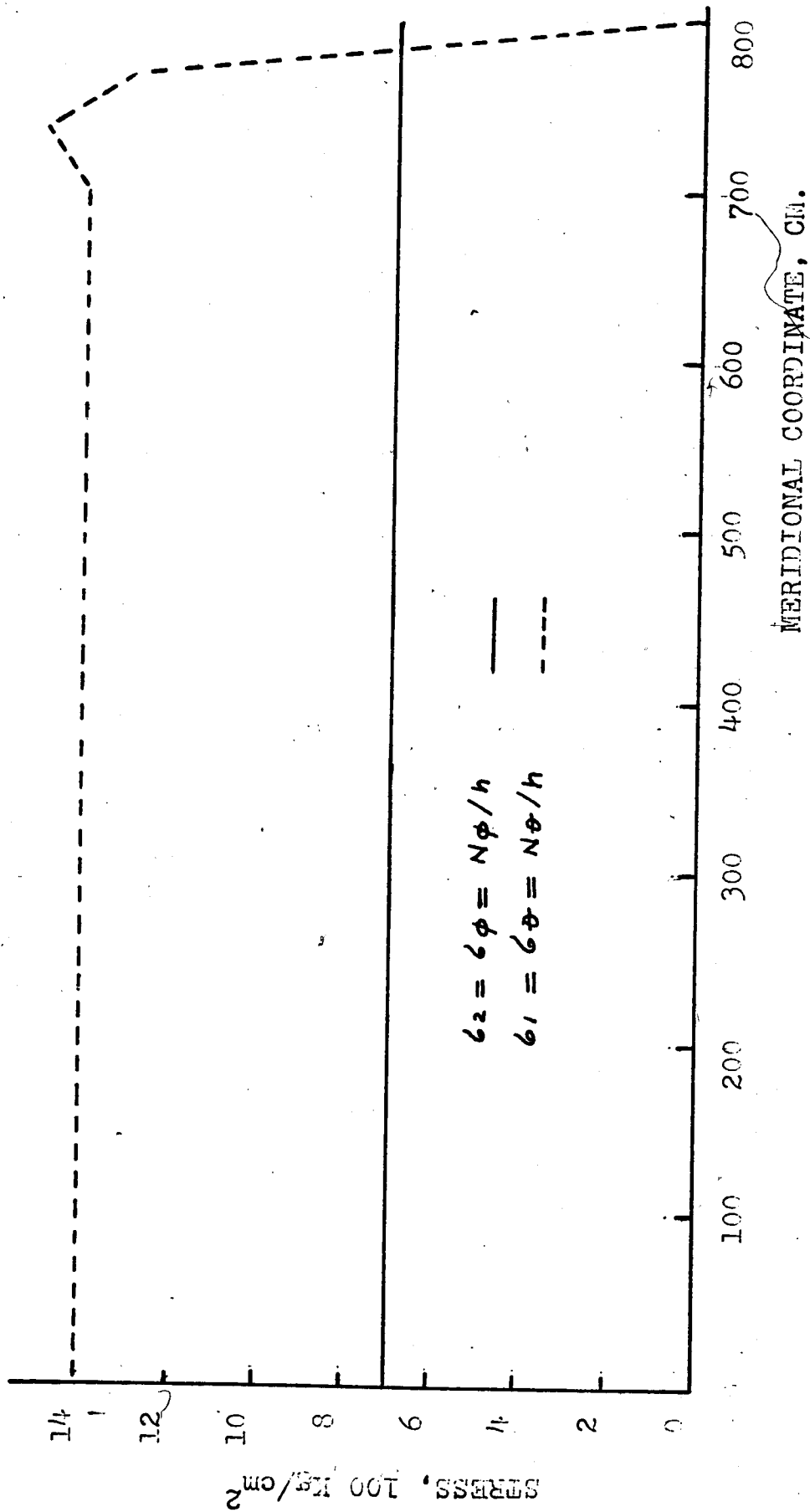


Figure 12-4. Membrane Stress in Cylindrical Surface.

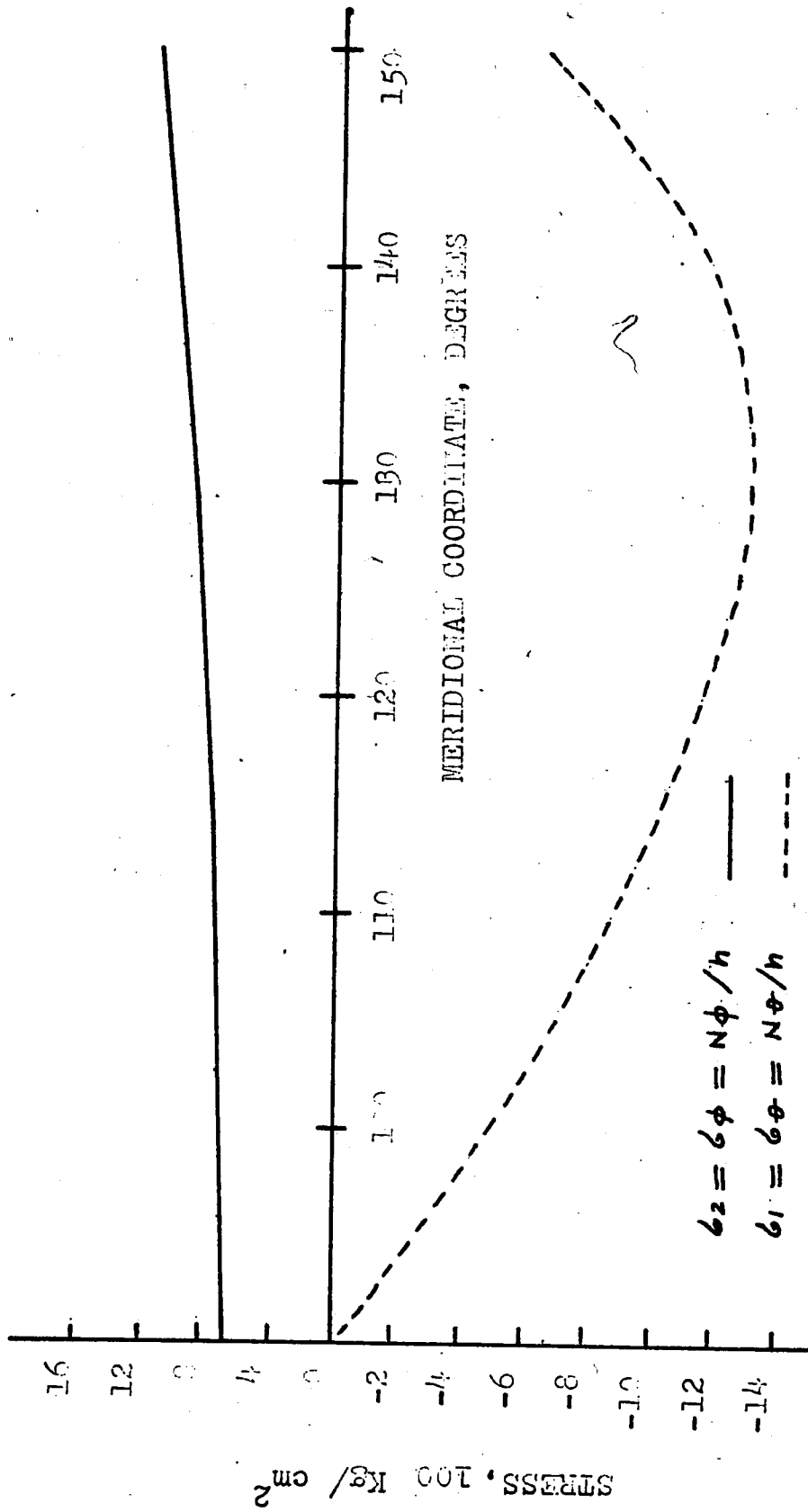


Figure 12-5. Membrane Stress in Toroidal Surface.

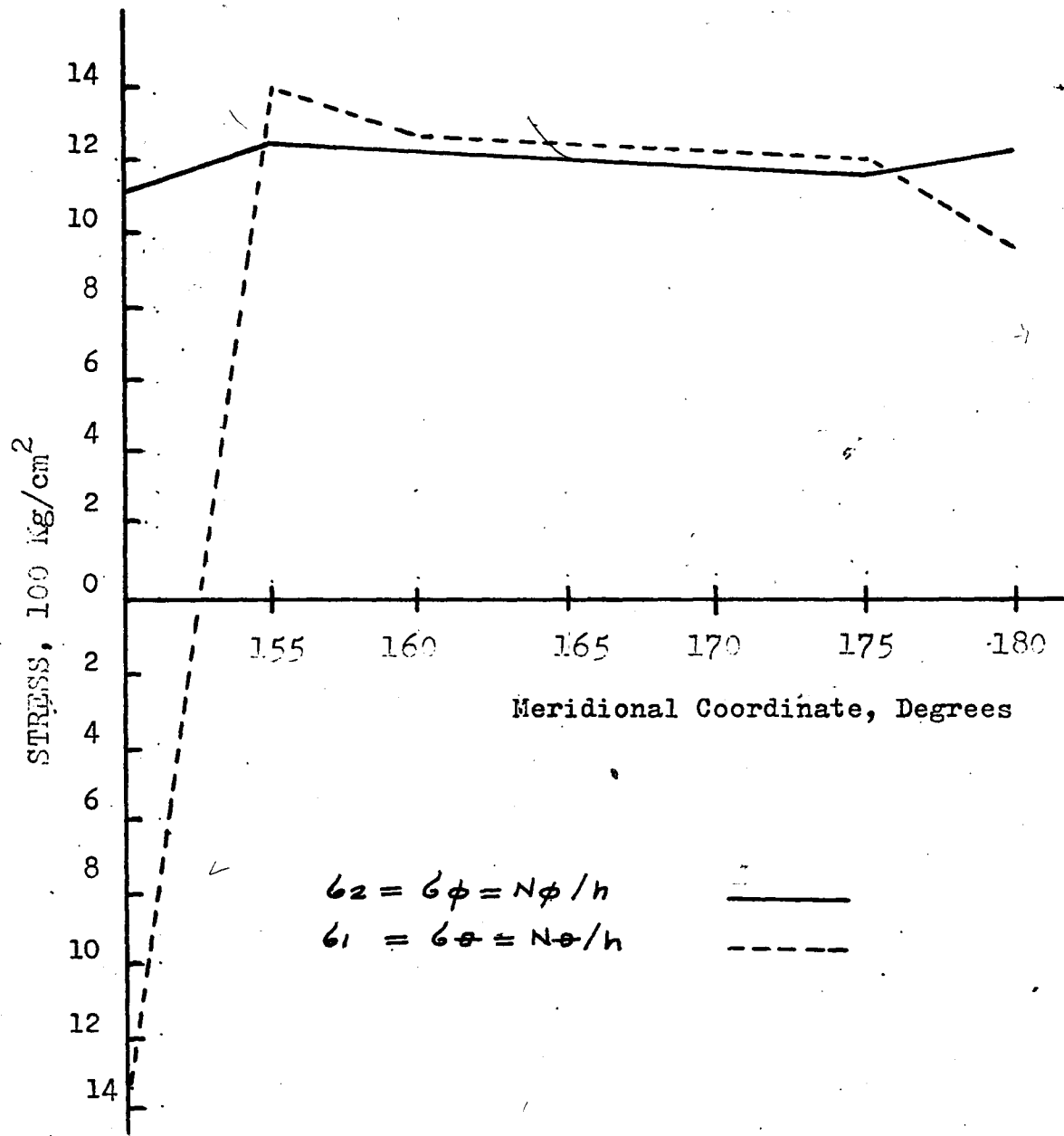


Figure 12-6. Membrane Stress in Spherical Surface

GLOSSARY OF COMPUTER PROGRAM

PART No 1	Cylindrical Surface
PART No 2	Toroidal Surface
PART No 3	Spherical Surface
M	Meridional Coordinate. Distance M along generator in Cylindrical Surfaces.
	Meridional coordinate in degrees in toroidal and spherical surfaces.
ϕ	Angle between normal and axis of symmetry for shell of revolution; circumferential angle for torus.
	Displacement in normal direction
Q	Transverse shear resultant force in normal direction
$U_{PHI} = u_{\phi}$	Displacement in meridional direction.
$H_{PHI} = N_{\phi}$	Resultant force in meridional direction
$B_{PHI} = \beta_{\phi}$	Angle of rotation of the normal in meridional direction
$U_{THETA} = u_{\theta}$	Displacement in circumferential direction
H	Circumferential shear force
$M_{PHI} = M_{\phi}$	Meridional bending moment

$$M_{\theta} = N_{\theta}$$

$$M_{\theta} = M_{\theta}$$

θ

ϕ

θ

ν

Parameters

Equivalent stress in circumferential direction

Circumferential bending moment

Circumferential angle for shell of revolution; axial angle for torus

Membrane stress in meridional

$$\text{direction} (= N_{\phi} / h \pm 6 M_{\phi} / h^2)$$

Membrane stress in circumferential

$$\text{direction} (= N_{\theta} / h \pm 6 M_{\theta} / h^2)$$

Local thickness

Young's modulus

Poisson's ratio

See Page

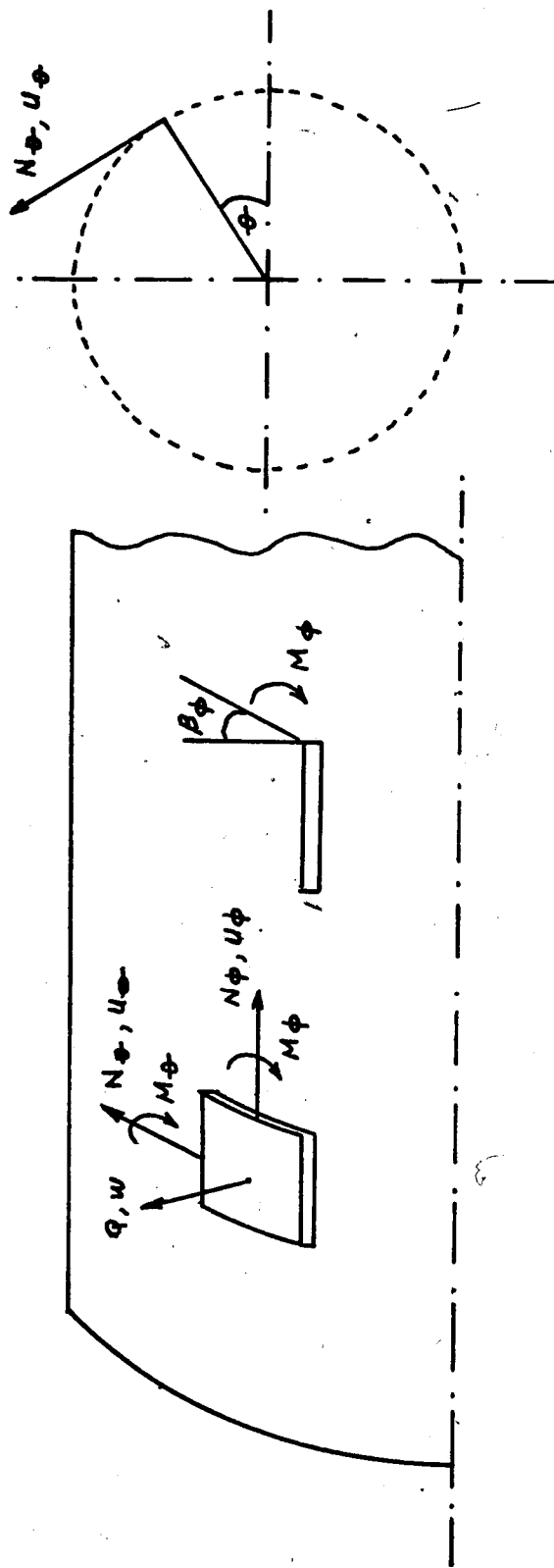


Figure 12-7. Parameters of Computer Program.

TABLE 12-1. KSHELL FOR ANALYSIS OF AXISYMMETRIC SHELLS, BY ARTURS KALNINS, SEPT 1, 1974

DEFLECTIONS AND STRESS RESULTANTS FOR SUBCASE NO. 1 N= 0 TORI-SPHERICAL VESSEL

X	W	Q	UPHI	NPHI	BPFI	MPHI	UTHETA
MAIN SHELL PART NO 1							
0.0000	1.38340E-01	0.	0.	6.99129E+02	0.	-3.64900E-02	0.
14.2857	1.38343E-01	6.50229E-03	1.15906E-03	6.99129E+02	-5.95746E-07	-8.42092E-02	0.
28.5714	1.38361E-01	1.00093E-02	2.31801E-03	6.99129E+02	-2.20695E-06	-2.08729E-01	0.
28.5714	1.38345E-01	-2.78844E-03	2.31776E-03	6.99129E+02	-1.26627E-07	4.30070E-03	0.
42.8571	1.38348E-01	-7.67154E-03	3.47676E-03	6.99129E+02	-4.40964E-07	-7.14470E-02	0.
57.1429	1.38363E-01	-1.01689E-02	4.63568E-03	6.99129E+02	-1.96892E-06	-2.04384E-01	0.
57.1429	1.38347E-01	-3.18307E-03	4.63544E-03	6.99129E+02	-2.16375E-08	2.85608E-04	0.
71.4285	1.38349E-01	-7.57758E-03	5.79442E-03	6.99129E+02	-3.53389E-07	-7.69880E-02	0.
85.7143	1.38363E-01	-9.97589E-03	6.95334E-03	6.99129E+02	-1.93244E-06	-2.07592E-01	0.
85.7143	1.38347E-01	-3.00615E-03	6.95310E-03	6.99129E+02	5.34078E-08	-3.40207E-03	0.
100.0000	1.38348E-01	-7.44603E-03	8.11208E-03	6.99129E+02	-3.49885E-07	-7.83994E-02	0.
114.2857	1.38363E-01	-9.91178E-03	9.27100E-03	6.99129E+02	-1.93576E-06	-2.07587E-01	0.
114.2857	1.38347E-01	-2.94990E-03	9.27076E-03	6.99129E+02	4.73150E-08	-3.66148E-03	0.
128.5714	1.38348E-01	-7.43175E-03	1.04297E-02	6.99129E+02	-3.55683E-07	-7.81880E-02	0.
142.8571	1.38363E-01	-9.91498E-03	1.15887E-02	6.99129E+02	-1.93861E-06	-2.07319E-01	0.
142.8571	1.38347E-01	-2.95414E-03	1.15884E-02	6.99129E+02	4.40955E-08	-3.42905E-03	0.
157.1429	1.38348E-01	-7.43863E-03	1.27474E-02	6.99129E+02	-3.56740E-07	-7.80449E-02	0.
171.4286	1.38363E-01	-9.91953E-03	1.39063E-02	6.99129E+02	-1.93855E-06	-2.07260E-01	0.
171.4286	1.38347E-01	-2.95886E-03	1.39061E-02	6.99129E+02	4.40820E-08	-3.37617E-03	0.
185.7143	1.38348E-01	-7.44061E-03	1.50651E-02	6.99129E+02	-3.56457E-07	-7.80390E-02	0.
200.0000	1.38363E-01	-9.91989E-03	1.62240E-02	6.99129E+02	-1.93831E-06	-2.07269E-01	0.

X	N	NTHETA	NTHETA
0.0000	0.	1.39981E+03-1.09470E-02	
14.2857	0.	1.39984E+03-2.52628E-02	
28.5714	0.	1.40000E+03-6.26187E-02	
28.5714	0.	1.39985E+03 1.29021E-03	
42.8571	0.	1.39988E+03-2.14341E-02	
57.1429	0.	1.40001E+03-6.13152E-02	
57.1429	0.	1.39987E+03 8.56824E-05	
71.4286	0.	1.39989E+03-2.30964E-02	
85.7143	0.	1.40001E+03-6.22777E-02	
85.7143	0.	1.39987E+03-1.02062E-03	
100.0000	0.	1.39988E+03-2.35198E-02	
114.2857	0.	1.40001E+03-6.22760E-02	
114.2857	0.	1.39987E+03-1.09845E-03	
128.5714	0.	1.39988E+03-2.34564E-02	
142.8571	0.	1.40001E+03-6.21957E-02	
142.8571	0.	1.39987E+03-1.02872E-03	
157.1429	0.	1.39988E+03-2.34135E-02	
171.4286	0.	1.40001E+03-6.21779E-02	
171.4286	0.	1.39987E+03-1.01285E-03	
185.7143	0.	1.39988E+03-2.34117E-02	
200.0000	0.	1.40001E+03-6.21807E-02	

X	M	Q	UPHI	NPHI	BPHI	MPHI	UTHETA
200.0000	1.38347E-01	-2.95923E-03	1.62237E-02	6.99129E+02	4.43205E-08	-3.38579E-03	0.
214.2857	1.38348E-01	-7.44037E-03	1.73827E-02	6.99129E+02	3.56336E-07	-7.80487E-02	0.
228.5714	1.38363E-01	-9.91959E-03	1.85417E-02	6.99129E+02	-1.93827E-06	-2.07274E-01	0.
228.5714	1.38347E-01	-2.95893E-03	1.85414E-02	6.99129E+02	4.43566E-08	-3.39115E-03	0.
242.8571	1.38348E-01	-7.44019E-03	1.97004E-02	6.99129E+02	3.56339E-07	-7.80505E-02	0.
257.1429	1.38363E-01	-9.91952E-03	2.08593E-02	6.99129E+02	-1.93829E-06	-2.07275E-01	0.
257.1429	1.38347E-01	-2.95886E-03	2.08591E-02	6.99129E+02	4.43442E-08	-3.39123E-03	0.
271.4286	1.38348E-01	-7.44018E-03	2.20181E-02	6.99129E+02	3.56349E-07	-7.80501E-02	0.
285.7143	1.38363E-01	-9.91953E-03	2.31770E-02	6.99129E+02	-1.93829E-06	-2.07274E-01	0.
285.7143	1.38347E-01	-2.95887E-03	2.31767E-02	6.99129E+02	4.43390E-08	-3.39089E-03	0.
300.0000	1.38348E-01	-7.44019E-03	2.43357E-02	6.99129E+02	3.56351E-07	-7.80499E-02	0.
314.2857	1.38363E-01	-9.91953E-03	2.54946E-02	6.99129E+02	-1.93829E-06	-2.07274E-01	0.
314.2857	1.38347E-01	-2.95887E-03	2.54944E-02	6.99129E+02	4.43377E-08	-3.39080E-03	0.
328.5714	1.38348E-01	-7.44017E-03	2.66534E-02	6.99129E+02	3.56351E-07	-7.80497E-02	0.
342.8571	1.38363E-01	-9.91949E-03	2.78123E-02	6.99129E+02	-1.93829E-06	-2.07273E-01	0.
342.8571	1.38347E-01	-2.95883E-03	2.78121E-02	6.99129E+02	4.43438E-08	-3.39006E-03	0.
357.1429	1.38348E-01	-7.44014E-03	2.89711E-02	6.99129E+02	3.56333E-07	-7.80484E-02	0.
371.4286	1.38363E-01	-9.91956E-03	3.01300E-02	6.99129E+02	-1.93826E-06	-2.07272E-01	0.
371.4286	1.38347E-01	-2.95889E-03	3.01297E-02	6.99129E+02	4.43760E-08	-3.38896E-03	0.
385.7143	1.38348E-01	-7.44044E-03	3.12887E-02	6.99129E+02	3.56299E-07	-7.80497E-02	0.
400.0000	1.38363E-01	-9.92021E-03	3.24476E-02	6.99129E+02	-1.93827E-06	-2.07280E-01	0.
400.0000	1.38347E-01	-2.95955E-03	3.24474E-02	6.99129E+02	4.43625E-08	-3.39695E-03	0.
414.2857	1.38348E-01	-7.44136E-03	3.36064E-02	6.99129E+02	3.56466E-07	-7.80693E-02	0.
428.5714	1.38363E-01	-9.92061E-03	3.47653E-02	6.99129E+02	-1.93873E-06	-2.07311E-01	0.
428.5714	1.38347E-01	-2.95995E-03	3.47651E-02	6.99129E+02	4.39044E-08	-3.42757E-03	0.
442.8571	1.38348E-01	-7.43918E-03	3.59240E-02	6.99129E+02	3.57250E-07	-7.80903E-02	0.
457.1429	1.38363E-01	-9.91257E-03	3.77830E-02	6.99129E+02	-1.93944E-06	-2.07263E-01	0.

X	N	NTHETA	MIHETA
200.0000	0.	1.39987E+03-1.	0.01574E-03
214.2857	0.	1.39988E+03-2.	34146E-02
228.5714	0.	1.40001E+03-6.	21823E-02
228.5714	0.	1.39987E+03-1.	0.01734E-03
242.8571	0.	1.39988E+03-2.	34152E-02
257.1429	0.	1.40001E+03-6.	21824E-02
257.1429	0.	1.39987E+03-1.	0.01737E-03
271.4286	0.	1.39988E+03-2.	34150E-02
285.7143	0.	1.40001E+03-6.	21823E-02
285.7143	0.	1.39987E+03-1.	0.01727E-03
300.0000	0.	1.39988E+03-2.	34150E-02
314.2857	0.	1.40001E+03-6.	21822E-02
314.2857	0.	1.39987E+03-1.	0.01724E-03
328.5714	0.	1.39988E+03-2.	34149E-02
342.8571	0.	1.40001E+03-6.	21820E-02
342.8571	0.	1.39987E+03-1.	0.01702E-03
357.1429	0.	1.39988E+03-2.	34145E-02
371.4286	0.	1.40001E+03-6.	21817E-02
371.4286	0.	1.39987E+03-1.	0.01669E-03
385.7143	0.	1.39988E+03-2.	34149E-02
400.0000	0.	1.40001E+03-6.	21841E-02
400.0000	0.	1.39987E+03-1.	0.01909E-03
414.2857	0.	1.39988E+03-2.	34208E-02
428.5714	0.	1.40001E+03-6.	21933E-02
428.5714	0.	1.39987E+03-1.	0.02827E-03
442.8571	0.	1.39988E+03-2.	34271E-02
457.1429	0.	1.40001E+03-6.	21790E-02

X	W	Q	UPHI	NPHI	8PHI	MPHI	UTHETA
457.	1429	1.38347E-01-2	.95192E-03	3.70827E-02	6.99129E+02	4.31831E-08-3	.38062E-03 0.
471.	4286	1.38348E-01-7	.42259E-03	3.82417E-02	6.99129E+02	3.56565E-07-7	.78685E-02 0.
485.	7143	1.38363E-01-9	.89141E-03	3.94006E-02	6.99129E+02	1.93471E-06-2	.06759E-01 0.
485.	7143	1.38347E-01-2	.93076E-03	3.94004E-02	6.99129E+02	4.79111E-08-2	.87698E-03 0.
500.	0000	1.38348E-01-7	.41826E-03	4.05594E-02	6.99129E+02	3.44592E-07-7	.71343E-02 0.
514.	2857	1.38363E-01-9	.95755E-03	4.17183E-02	6.99129E+02	1.91579E-06-2	.06403E-01 0.
514.	2857	1.38347E-01-2	.99679E-03	4.17181E-02	6.99129E+02	6.69126E-08-2	.51495E-03 0.
528.	5714	1.38348E-01-7	.63349E-03	4.28770E-02	6.99129E+02	3.30306E-07-7	.86841E-02 0.
542.	8571	1.38362E-01-1	.03716E-02	4.40360E-02	6.99129E+02	1.94171E-06-2	.12443E-01 0.
542.	8571	1.38346E-01-3	.41098E-03	4.40357E-02	6.99129E+02	4.08808E-08-8	.56309E-03 0.
557.	1429	1.38348E-01-8	.10805E-03	4.51947E-02	6.99129E+02	4.62042E-07-9	.14511E-02 0.
571.	4286	1.38366E-01-1	.03012E-02	4.63536E-02	6.99129E+02	2.24787E-06-2	.29205E-01 0.
571.	4286	1.38350E-01-3	.34077E-03	4.63534E-02	6.99129E+02	2.65523E-07-2	.53421E-02 0.
585.	7143	1.38357E-01-6	.15595E-03	4.75123E-02	6.99129E+02	9.13850E-07-9	.58563E-02 0.
600.	0000	1.38380E-01-4	.60146E-03	4.86711E-02	6.99129E+02	2.50343E-06-1	.81143E-01 0.
600.	0000	1.38364E-01	2.35837E-03	4.86709E-02	6.99129E+02	5.19833E-07	2.27929E-02 0.
614.	2857	1.38369E-01	4.06718E-03	4.98296E-02	6.99129E+02	3.44412E-08	6.69936E-02 0.
628.	5714	1.38362E-01	5.68678E-03	5.09884E-02	6.99129E+02	1.11063E-06	1.39069E-01 0.
628.	5714	1.38346E-01	1.26465E-02	5.09882E-02	6.99129E+02	3.09266E-06	3.42915E-01 0.
642.	8571	1.38270E-01-2	.01851E-03	5.21475E-02	6.99129E+02	7.76162E-06	4.46613E-01 0.
657.	1429	1.38128E-01-5	.05821E-02	5.33080E-02	6.99129E+02	1.16453E-05	1.23442E-01 0.
657.	1429	1.38112E-01-4	.35938E-02	5.33078E-02	6.99129E+02	1.36257E-05	3.27512E-01 0.
671.	4286	1.37916E-01-1	.51262E-01	5.44704E-02	6.99129E+02	1.13180E-05	9.91659E-01 0.
685.	7143	1.37907E-01-2	.99591E-01	5.56344E-02	6.99129E+02	1.61158E-05	4.20638E+00 0.
685.	7143	1.37891E-01-2	.92546E-01	5.56341E-02	6.99129E+02	1.41176E-05	4.00067E+00 0.
700.	0000	1.38542E-01-3	.63659E-01	5.67954E-02	6.99129E+02	8.63402E-05	8.92253E+00 0.
714.	2857	1.40624E-01-3	.48492E-02	5.79428E-02	6.99129E+02	2.12255E-04	1.25290E+01 0.

X	N	NTHETA	NIHETA
457.1429	0.	1.39987E+03-1.01418E-03	
471.4285	0.	1.39988E+03-2.33605E-02	
485.7143	0.	1.40001E+03-6.20277E-02	
485.7143	0.	1.39987E+03-8.63094E-04	
500.0000	0.	1.39988E+03-2.31403E-02	
514.2857	0.	1.40001E+03-6.19209E-02	
514.2857	0.	1.39987E+03-7.54485E-04	
528.5714	0.	1.39988E+03-2.36052E-02	
542.8571	0.	1.40000E+03-6.37329E-02	
542.8571	0.	1.39987E+03-2.56893E-03	
557.1429	0.	1.39988E+03-2.74353E-02	
571.4286	0.	1.40003E+03-6.87616E-02	
571.4286	0.	1.39990E+03-7.60263E-03	
585.7143	0.	1.39996E+03-2.87569E-02	
600.0000	0.	1.40016E+03-5.43430E-02	
600.0000	0.	1.40002E+03 6.83786E-03	
614.2857	0.	1.40006E+03 2.00981E-02	
628.5714	0.	1.40000E+03 4.17208E-02	
628.5714	0.	1.39987E+03 1.02875E-01	
642.8571	0.	1.39921E+03 1.33984E-01	
657.1429	0.	1.39798E+03 3.70327E-02	
657.1429	0.	1.39785E+03 9.82535E-02	
671.4285	0.	1.39616E+03-2.97498E-01	
685.7143	0.	1.39609E+03-1.26192E+00	
685.7143	0.	1.39595E+03-1.20020E+00	
700.0000	0.	1.40155E+03-2.67676E+00	
714.2857	0.	1.41946E+03-3.75869E+00	

X	W	Q	UPHI	NPHI	8PHI	MPHI	UTHETA	
714.	2857	1.40607E-01-2.80740E-02	5.79426F-02	6.99129E+02-2.10201E-04-1.23230E+01	0.			
728.	5714	1.44534E-01	1.22147E+00	5.90578E-02	6.99129E+02-3.26533E-04-5.24154E+00	0.		
742.	8571	1.48943E-01	3.82994E+00	6.01257E-02	6.99129E+02-2.26062E-04	2.92009E+01	0.	
742.	8571	1.48925E-01	3.83542E+00	6.01255E-02	6.99129E+02-2.24135E-04	2.93852E+01	0.	
757.	1429	1.47943E-01	7.19668E+00	6.11671F-02	6.99129E+02	5.11259E-04	1.08489E+02	0.
771.	4286	1.28854E-01	7.80161E+00	6.23017E-02	6.99129E+02	2.38002E-03	2.23169E+02	0.
771.	4286	1.28849F-01	7.89815E+00	6.23015E-02	6.99129E+02	2.38094E-03	2.23308E+02	0.
785.	7143	7.42117E-02-2.30980E+00	6.38163F-02	6.99129E+02	5.38693E-03	2.83186E+02	0.	
800.	0000-2.24187E-02-3.59914E+01	6.61497E-02	6.99129E+02	7.70093E-03	4.51579E+01	0.		
MAIN SHELL PART NO 2								
90.	0000-2.23794F-02-3.59649E+01	6.61488E-02	6.99129E+02	7.70158E-03	4.54961E+01	0.		
93.	3333-6.30431E-02-1.81539E+01	6.99128E-02	7.01074E+02	7.51550E-03-1.09291E+02	0.			
96.	6667-1.09689E-01-5.64596E+00	7.61622E-02	7.03355E+02	6.83141E-03-1.76206E+02	0.			
96.	6667-1.00689E-01-5.64713F+00	7.61628E-02	7.03356E+02	6.83135E-03-1.76217E+02	0.			
100.	0000-1.33323E-01	2.14498E+00	8.46400E-02	7.06833E+02	5.98536E-03-1.84569E+02	0.		
103.	3333-1.60551E-01	5.99939F+00	9.50177E-02	7.12220E+02	5.18758E-03-1.59515E+02	0.		
103.	3333-1.60548F-01	5.99893F+00	9.50180E-02	7.12220E+02	5.18767E-03-1.59517E+02	0.		
106.	6667-1.82900E-01	6.71342E+00	1.06978F-01	7.20094E+02	4.54288E-03-1.21558E+02	0.		
110.	0000-2.01278F-01	5.01822E+00	1.20251E-01	7.30926E+02	4.07187E-03-8.67409E+01	0.		
110.	0000-2.01276F-01	5.01814E+00	1.20251E-01	7.30926E+02	4.07194F-03-8.67454E+01	0.		
113.	3333-2.16520E-01	1.55782E+00	1.34625E-01	7.45120E+02	3.73082E-03-6.71691E+01	0.		
116.	6667-2.29081E-01-3.07929E+00	1.49932F-01	1.49932F-01	7.63035E+02	3.42810E-03-7.14317E+01	0.		
116.	6667-2.29080E-01-3.07952F+00	1.49932F-01	1.49932F-01	7.63035E+02	3.42813E-03-7.14368E+01	0.		
120.	0000-2.38783E-01-8.30195E+00	1.66012E-01	1.66012E-01	7.84970E+02	3.04007E-03-1.04808E+02	0.		
123.	3333-2.44688E-01-1.34477E+01	1.82673F-01	1.82673F-01	8.11133E+02	2.42637E-03-1.69007E+02	0.		

X	N	NTHETA	MTHETA
714.2857	0.	1.41932E+03-3.69690E+00	
728.5714	0.	1.45309E+03-1.57246E+00	
742.8571	0.	1.49102E+03 8.76026E+00	
742.8571	0.	1.49087 +03 8.81556E+00	
757.1429	0.	1.48242E+03 3.25466E+01	
771.4286	0.	1.31821E+03 6.69508E+01	
771.4286	0.	1.31816E+03 6.69923E+01	
785.7143	0.	8.48147E+02 8.49559E+01	
800.0000	0.	1.68808E+01 1.35474E+01	
MAIN SHELL PART NO 2			
90.0000	0.	1.72185E+01 1.36488E+01	
93.3333	0.	-3.66304E+02-3.40408E+01	
96.6667	0.	-7.26966E+02-5.51398E+01	
96.6667	0.	-7.26968E+02-5.51430E+01	
100.0000	0.	-1.04867E+03-5.83623E+01	
103.3333	0.	-1.32915E+03-5.13082E+01	
103.3333	0.	-1.3291 +03-5.13089E+01	
106.6667	0.	-1.5740 +03-4.02433E+01	
110.0000	0.	-1.79193E+03-3.00769E+01	
110.0000	0.	-1.79191E+03-3.00783E+01	
113.3333	0.	-1.99073E+03-2.44765E+01	
116.6667	0.	-2.17493E+03-2.59618E+01	
116.6667	0.	-2.17492E+03-2.59634E+01	
120.0000	0.	-2.34390E+03-3.59521E+01	
123.3333	0.	-2.49131E+03-5.46894E+01	

X	W	Q	UPHI	NPHI	BPHI	MPHI	UTHEYA
123.	3333-2.44689E-01-1.34478E+01	1.82673E-01	8.11133E+02	2.42644E-03-1.69006E+02	0.		
126.	6667-2.45046E-01-1.77260E+01	1.99642E-01	8.41567E+02	1.44764E-03-2.61605E+02	0.		
130.	0000-2.37365E-01-2.01856E+01	2.16513E-01	8.76069E+02-1.38453E-05-3.75134E+02	0.			
130.	0000-2.37367E-01-2.01858E+01	2.16513E-01	8.76069E+02-1.37191E-05-3.75130E+02	0.			
133.	3333-2.18629E-01-1.97251E+01	2.32709E-01	9.14100E+02-2.02806E-03-4.96106E+02	0.			
136.	6667-1.85652E-01-1.51508E+01	2.47460E-01	9.54719E+02-4.58817E-03-6.04220E+02	0.			
136.	6667-1.85655E-01-1.51513E+01	2.47461E-01	9.54719E+02-4.58798E-03-6.04217E+02	0.			
140.	0000-1.75656E-01-5.28861E+00	2.59814E-01	9.96571E+02-7.57666E-03-6.72014E+02	0.			
143.	3333-6.69913E-02	1.08693E+01	2.68675E-01	1.03794E+03-1.07337E-02-6.65288E+02	0.		
143.	3333-6.69966E-02	1.08694E+01	2.68676E-01	1.03794E+03-1.07335E-02-6.65291E+02	0.		
146.	6667	1.99075E-02	3.39916E+01	2.72912E-01	1.07693E+03-1.36264E-02-5.44442E+02	0.	
150.	0000	1.21492E-01	6.42628E+01	2.71508E-01	1.11170E+03-1.56294E-02-2.66746E+02	0.	
MAIN SHELL PART NO 3							
150.	0000	1.21490E-01	6.42617E+01	2.71510E-01	1.11171E+03-1.56293E-02-2.66757E+02	0.	
151.	4000	3.95334E-01	1.57473E+01	2.72018E-01	1.19395E+03-1.41760E-02	3.76076E+02	0.
152.	8000	5.96031E-01-5.83488E+00	2.65238E-01	1.23397E+03-8.37472E-03	4.41565E+02	0.	
152.	8000	5.96048E-01-5.82482E+00	2.65236E-01	1.23395E+03-8.37340E-03	4.41760E+02	0.	
154.	2000	6.99907E-01-1.06180E+01	2.53857E-01	1.24434E+03-3.35158E-03	2.96861E+02	0.	
155.	6000	7.35604E-01-6.19180E+00	2.40417E-01	1.24014E+03-4.68080E-04	1.38318E+02	0.	
155.	6000	7.35568E-01-6.18109E+00	2.40415E-01	1.24012E+03-4.64996E-04	1.38686E+02	0.	
157.	0000	7.37736E-01-4.32740E+00	2.26453E-01	1.23194E+03	6.48176E-04	3.52782E+01	0.
158.	4000	7.30083E-01-1.45215E+00	2.12614E-01	1.22500E+03	7.68714E-04-1.16405E+01	0.	
158.	4000	7.30080E-01-1.45235E+00	2.12614E-01	1.22500E+03	7.69480E-04-1.15615E+01	0.	
159.	8000	7.23845E-01	2.90787E-02	1.99013E-01	1.22075E+03	5.22332E-04-2.26156E+01	0.
161.	2000	7.22057E-01	5.00923E-01	1.85557E-01	1.21874E+03	2.46031E-04-1.79135E+01	0.

X	N	NTHETA	NIHETA
123.3333	0.	-2.49131E+03-5	46892E+01
126.6667	0.	-2.60537E+03-8	10893E+01
130.0000	0.	-2.67017E+03-1	12513E+02
133.3333	0.	-2.67019E+03-1	12512E+02
136.6667	0.	-2.66810E+03-1	44549E+02
136.6667	0.	-2.58307E+03-1	70882E+02
136.6667	0.	-2.58309E+03-1	70881E+02
140.0000	0.	-2.40476E+03-1	83329E+02
143.3333	0.	-2.13285E+03-1	72133E+02
143.3333	0.	-2.13289E+03-1	72135E+02
146.6667	0.	-1.78132E+03-1	26544E+02
150.0000	0.	-1.38097E+03-3	56662E+01
/ MAIN SHELL PART NO 3			
150.0000	0.	-1.38099E+03-3	56695E+01
151.4000	0.	-1.51008E+02	1.55427E+02
152.8000	0.	7.63114E+02	1.59171E+02
152.8000	0.	7.63218E+02	1.59225E+02
154.2000	0.	1.23246E+03	1.00419E+02
155.6000	0.	1.38274E+03	4.31862E+01
155.6000	0.	1.38259E+03	4.32854E+01
157.0000	0.	1.37359E+03	8.08134E+00
158.4000	0.	1.31663E+03-6	67355E+00
158.4000	0.	1.31661E+03-6	65300E+00
159.8000	0.	1.26551E+03-9	11090E+00
161.2000	0.	1.23563E+03-6	55826E+00

X	M	Q	UPHI	NPHI	BPFI	MPHI	UTHETA
161.	2000	7.22050E-01	5.04061E-01	1.85556E-01	1.21873E+03	2.47487E-04	-1.78026E+01
162.	6000	7.23924E-01	4.65473E-01	1.72120E-01	1.21795E+03	6.43053E-05	-9.74500E+00
164.	0000	7.27709E-01	2.69624E-01	1.58617E-01	1.21751E+03	-2.35175E-05	-3.76269E+00
164.	0000	7.27697E-01	2.76369E-01	1.58615E-01	1.21749E+03	-2.13702E-05	-3.57191E+00
165.	4000	7.32051E-01	1.00095E-01	1.45005E-01	1.21679E+03	-4.72969E-05	-5.76719E-01
166.	8000	7.36271E-01	5.19062E-03	1.31276E-01	1.21544E+03	-4.98350E-05	1.54356E-01
166.	8000	7.36260E-01	1.49493E-02	1.31274E-01	1.21540E+03	-4.71224E-05	4.17425E-01
168.	2000	7.40064E-01	1.30520E-02	1.17430E-01	1.21304E+03	-4.21688E-05	5.26198E-01
169.	6000	7.43417E-01	1.02871E-01	1.03473E-01	1.20918E+03	-3.22049E-05	1.42250E+00
169.	6000	7.43408E-01	1.19330E-01	1.03469E-01	1.20908E+03	-2.79245E-05	1.85036E+00
171.	0000	7.45921E-01	2.85150E-01	8.94033E-02	1.20287E+03	1.83466E-05	5.57906E+00
172.	4000	7.46697E-01	4.33094E-01	7.52478E-02	1.19331E+03	1.44326E-04	1.30940E+01
172.	4000	7.46702E-01	4.50893E-01	7.52428E-02	1.19318E+03	1.48439E-04	1.35323E+01
173.	8000	7.47338E-01	2.94385E-01	6.10531E-02	1.17963E+03	4.20389E-04	2.41805E+01
175.	2000	7.34383E-01	-8.87174E-01	4.69673E-02	1.16450E+03	8.47385E-04	2.92055E+01
175.	2000	7.34436E-01	-8.58557E-01	4.69593E-02	1.16415E+03	8.51745E-04	2.98140E+01
176.	6000	7.17056E-01	-4.60017E+00	3.32303E-02	1.16093E+03	1.24778E-03	2.20341E+00
178.	0000	6.98428E-01	-1.48232E+01	2.02897E-02	1.24079E+03	6.70343E-04	-1.51449E+02

X	N	NTHETA	MIHETA
161.2000	0.	1.23560E+03-6	53201E+00
162.6000	0.	1.22400E+03-3	25973E+00
164.0000	0.	1.22327E+03-9	94417E-01
164.0000	0.	1.22323E+03-9	49455E-01
165.4000	0.	1.22709E+03	1.24511E-01
166.8000	0.	1.23259E+03	3.94461E-01
166.8000	0.	1.23258E+03	4.54431E-01
168.2000	0.	1.23870E+03	4.88609E-01
169.6000	0.	1.24578E+03	7.14275E-01
169.6000	0.	1.24583E+03	8.04418E-01
171.0000	0.	1.25280E+03	1.48391E+00
172.4000	0.	1.25627E+03	2.15577E+00
172.4000	0.	1.25644E+03	2.23675E+00
173.8000	0.	1.24722E+03	9.13183E-01
175.2000	0.	1.20988E+03-7	77386E+00
175.2000	0.	1.21050E+03-7	67639E+00
176.6000	0.	1.12356E+03-3	37539E+01
178.0000	0.	9.4927 E+02-7	68902E+01

Antonio Serrano, son of Mr. & Mrs. Antonio Serrano, was born on June 12, 1937 in Bucaramanga, Colombia. From 1957 to 1963 he attended the Industrial University of Santander, Bucaramanga, for a full-time course in Mechanical Engineering, and graduated in Mechanical Engineering in December 1963. He worked as an Engineer with the Venezuelan Petrochemical Institute of Caracas, Venezuela from March 1965 to July 1974. He joined the Graduate School of Lehigh University, in the Department of Mechanical Engineering in January 1975. After June 1976, He will continue working for the Venezuelan Petrochemical Institute at their Central Engineering Offices at Caracas, Venezuela.